JPn

Neuroscience

The Journal of Physiology

Adenosine modulates light responses of rat retinal ganglion cell photoreceptors through a cAMP-mediated pathway

Puneet Sodhi[1] and Andrew T. E. Hartwick[2]

[1] *Department of Neuroscience, Ohio State University, Columbus, OH 43210, USA*
[2] *College of Optometry, Ohio State University, Columbus, OH 43210, USA*

Key points

- Melanopsin-containing ganglion cell photoreceptors are post-synaptic neurons and their light responses could therefore be modified by extracellular neuromodulators present in the mammalian retina.
- In this study, we show that the duration of light-evoked spiking in these intrinsically photoreceptive retinal ganglion cells (ipRGCs) is significantly lengthened following elevation of intracellular cyclic AMP (cAMP) levels.
- Furthermore, we demonstrate that adenosine, a retinal neuromodulator released at night and after dark adaptation, significantly reduced light-evoked ipRGC spiking through suppression of the cAMP-related pathway.
- The effects of adenosine were mediated through activation of A_1 receptors present on ipRGCs.
- Adenosine-mediated modulation of ipRGCs may represent an internal regulatory mechanism that influences a variety of light-regulated processes such as circadian rhythm photoentrainment, pupil constriction and sleep/wakefulness.

Abstract Adenosine is an established neuromodulator in the mammalian retina, with A_1 adenosine receptors being especially prevalent in the innermost ganglion cell layer. Activation of A_1 receptors causes inhibition of adenylate cyclase, decreases in intracellular cyclic AMP (cAMP) levels and inhibition of protein kinase A (PKA). In this work, our aim was to characterize the effects of adenosine on the light responses of intrinsically photosensitive retinal ganglion cells (ipRGCs) and to determine whether these photoreceptors are subject to neuromodulation through intracellular cAMP-related signalling pathways. Using multielectrode array recordings from postnatal and adult rat retinas, we demonstrated that adenosine significantly shortened the duration of ipRGC photoresponses and reduced the number of light-evoked spikes fired by these neurons. The effects were A_1 adenosine receptor-mediated, and the expression of this receptor on melanopsin-containing ipRGCs was confirmed by calcium imaging experiments on isolated cells in purified cultures. While inhibition of the cAMP/PKA pathway by adenosine shortened ipRGC light responses, stimulation of this pathway with compounds such as forskolin had the opposite effect and lengthened the duration of ipRGC spiking. Our findings reveal that the modification of ipRGC photoresponses through a cAMP/PKA pathway is a general feature of rat ganglion cell photoreceptors, and this pathway can be inhibited through activation of A_1 receptors by adenosine. As adenosine levels in the retina rise at night, adenosinergic modulation of ipRGCs may serve as an internal regulatory mechanism to limit transmission of nocturnal photic signals by ipRGCs to the brain. Targeting retinal A_1 adenosine receptors for ipRGC inhibition represents a potential therapeutic target for sleep disorders and migraine-associated photophobia.

Abbreviations 8-Br-cAMP, 8-bromoadenosine-3′,5′-cyclic monophosphate sodium salt; 8-Br-cGMP, 8-bromo guanosine cyclic 3′,5′-monophosphate sodium salt; 8-pCPT-cGMP, 8-(4-chlorophenylthio) guanosine-3′, 5′-cyclic monophosphate; BSA, bovine serum albumin; cAMP, cyclic AMP; Cl-MECA, 1-[2-chloro-6-[[(3-iodophenyl)methyl]amino]-9*H*-purin-9-yl]-1-deoxy-*N*-methyl-β-D-ribofuranuronamide; CPA, N^6-cyclopentyladenosine; DPBS, Dulbecco's phosphate buffered solution; DPCPX, 8-cyclopentyl-1,3-dipropylxanthine; HBSS, Hank's buffered salt solution; HCN, hyperpolarization-activated cyclic nucleotide-gated channel; ipRGCs, intrinsically photosensitive retinal ganglion cells; MDL 12330A, ($\pm$)-*N*-[(1*R**,2*R**)-2-phenylcyclopentyl]-azacyclotridec-1-en-2-amine hydrochloride; MEA, multielectrode array; NMBPR, 6-*S*-[(4-nitrophenyl)methyl]-6-thioinosine; PKA, protein kinase A; PKG, protein kinase G; PKI 14–22 amide, protein kinase inhibitor-(14-22)-amide, myristoylated; RGC, retinal ganglion cell; Sp-5,6-DCl-cBIMPS, 5, 6-dichloro-1-β-D-ribofuranosylbenzimidazole-3′, 5′-cyclic monophosphorothioate, Sp-isomer; TRPC, canonical transient receptor potential channel; VGCC, voltage-gated calcium channel.

Introduction

Intrinsically photosensitive retinal ganglion cells (ipRGCs) represent a small subset of neurons in the mammalian inner retina that are classified as photoreceptors due to their ability to capture light and convert it into an electrical signal (see reviews by Do & Yau, 2010; Lucas, 2013). The inherent light sensitivity of ipRGCs is conferred by the expression of the photopigment melanopsin throughout their dendrites and somata (Provencio *et al.* 1998; Hattar *et al.* 2002). In comparison to the light responses of rod and cone photoreceptors in the outer retina, the temporal characteristics of ipRGC light responses are strikingly different. Light induces sustained depolarization and action potential firing in ipRGCs, in contrast to the transient hyperpolarizing light responses of rods and cones, and their sluggish melanopsin-dependent responses can persist for many seconds after light offset (Berson *et al.* 2002; Dacey *et al.* 2005; Hartwick *et al.* 2007).

ipRGCs are retinal output neurons and transmit signals to the brain via their axons, which exit the eye in bundles contained in the optic nerve. The brain regions innervated by ipRGCs are diverse (Hattar *et al.* 2006; Brown *et al.* 2010), but a common theme of known ipRGC functions is that these photoreceptors primarily act as irradiance detectors, signalling information regarding the amount of light present in the environment. Similar to other retinal ganglion cells (RGCs), but unlike rods and cones, ipRGCs are post-synaptic neurons that have extensive dendritic arbors (Berson *et al.* 2010) along which synaptic connections with retinal bipolar and amacrine cells occur (Belenky *et al.* 2003; Wong *et al.* 2007). This property affords ipRGCs the ability to integrate network signals within the retina and supports the premise that interactions between ipRGCs and other retinal neurons can modify the light responses of these ganglion cell photoreceptors. Modulation of information regarding ambient light levels that is transmitted by ipRGCs could have

profound influence on the variety of functions that are regulated by these cells, which include circadian rhythm photoentrainment, pupil constriction, sleep/wakefulness and even perceptual brightness discrimination (Do & Yau, 2010; Lucas, 2013).

In this work, we first tested the hypothesis that the unique temporal characteristics of ipRGC light responses are subject to modification by changes in internal levels of cyclic AMP (cAMP), an important secondary messenger in many physiological signalling pathways (Missale *et al.* 1998). Changes in internal cAMP levels modulate the light responses of *Drosophila* and *Limulus* photoreceptors (Chyb *et al.* 1999; Battelle, 2002), suggesting that this may be a common feature of invertebrate photoreception. As phylogenetic analyses of the melanopsin protein indicate that it is more homologous to these invertebrate opsins than to vertebrate rod/cone opsins (Koyanagi *et al.* 2005; Peirson & Foster, 2006), we postulated similar cAMP-dependent modulation of ipRGCs. This cyclic nucleotide has already been shown to play a role in network adaptation at the ganglion cell level in vertebrates, as alterations in non-photosensitive RGC spiking have been linked to the changes in internal cAMP levels during light exposure (Vaquero *et al.* 2001).

Second, we sought to identify an endogenous retinal neuromodulator capable of modifying ipRGC responses through a cAMP-mediated pathway. One candidate, dopamine, is known to alter neuronal cAMP levels through G protein-coupled pathways and recent evidence indicates that ipRGC light responses are indeed affected by this retinal neuromodulator (Van Hook *et al.* 2012). In this work, however, we instead focused on adenosine, another known G protein-coupled neuromodulator of the CNS. In contrast to dopamine, which is released after light stimulation (Iuvone *et al.* 1978; Nir *et al.* 2000), retinal adenosine levels are thought to rise at night and during prolonged darkness (Ribelayga & Mangel, 2005). Adenosine can be directly released into

the extracellular retinal milieu through nucleoside transporters, or formed after enzymatic conversion of ATP by extracellular ecto-nucleotidases (Housley *et al.* 2009). In the inner retina, Müller glial cells (Newman, 2001, 2003, 2004), cholinergeric ('starburst') amacrine cells (Neal & Cunningham, 1994) and possibly some ganglion cells (Newman, 2005) are thought to be the major sources of ATP that is subsequently converted to adenosine.

Activation of A_1 and A_3 adenosine receptors is typically linked to inhibition of the enzyme adenylate cyclase, which causes subsequent lowering of intracellular cAMP levels, while A_{2A} and A_{2B} receptor activation leads to increased cAMP generation (Fredholm *et al.* 2001). Adenosine receptors are found throughout the mammalian retina, with the A_1 receptor especially prevalent in the ganglion cell layer (Blazynski & Perez, 1991). Stimulation of A_1 adenosine receptors on non-photosensitive RGCs results in the inhibition of voltage-gated calcium channels and glutamate-induced calcium influx (Hartwick *et al.* 2004). This previous work indicates that adenosine suppresses excitatory neurotransmission at the ganglion cell level, but the effect of this neuromodulator on melanopsin-based irradiance detection by ipRGCs is currently unknown. Our goal here was to characterize the effects of extracellular adenosine, and intracellular changes in cAMP, on the inherent light responses of ganglion cell photoreceptors in the rat retina.

Methods

Multielectrode array (MEA) recordings from rat retinas

The Ohio State University Institutional Animal Care and Use Committee approved all procedures. Neonatal and adult Long Evans rats (Charles River, Wilmington, MA, USA), housed under a 12/12 h light/dark cycle, were killed by decapitation after isoflurane overexposure (by inhalation in a sealed container) and the eyes were enucleated. The adult animals were dark adapted for 1 h prior to enucleation and dissections were performed under dim red light (625 nm; DiCon LED, Richmond, CA, USA) to minimize rod/cone photobleaching. Enucleation of the neonatal animals occurred under standard room lighting conditions, and these retinal dissections were performed under a white microscope light. For both the neonatal and the adult animals, the eyes were hemisected and the posterior eyecup was pinned down in a Sylgard-coated (Dow Corning, Midland, MI, USA) dish containing Ames medium (Sigma-Aldrich, St Louis, MO, USA) supplemented with 10 mM Hepes (pH 7.4; Sigma-Aldrich). The vitreous was removed with a pair of curved forceps, by placing the forceps underneath the vitreous and pulling up from the optic nerve head. Using a paintbrush, each retina was transferred to a glass coverslip and

trimmed to obtain square retinal pieces, which were placed ganglion cell-side down in a chamber with a 60-electrode array (30 μm diameter, 200 μm inter-electrode spacing; Multi-Channel Systems, Reutlingen, Germany) and anchored with a weighted, circular nylon mesh (ALA Scientific Instruments, Farmingdale, NY, USA). The array-mounted retina from one eye was then placed onto a heated stage that was continuously superfused (1 ml min^{-1} flow rate), via a peristaltic pump (Gilson, Middleton, WI, USA), with Ames medium (10 mM Hepes, pH 7.4) that was bubbled with 100% oxygen and pre-heated through a perfusion cannula (PH-01, Multi-Channel Systems). The temperature of the Ames medium in the chamber was 32–34°C. The retinal piece from the second eye was stored on the array in Hibernate-A medium (Brain Bits, Springfield, IL, USA) supplemented with 2% B-27 (Life Technologies, Grand Island, NY, USA) and maintained in the dark until the recordings from the first retina were completed. After transfer to the stage, which occurred under dim red light (GBX-2 Safelight filters; Kodak, Pittsburgh, PA, USA), the retinas were perfused with the heated, oxygenated Ames medium for 1 h in the dark prior to the first light exposure.

The light stimuli (all 20 s in duration) were generated using a blue LED source (470 nm module, Colibri system; Zeiss, Oberkochen, Germany) that was delivered from above the microscope stage. The Colibri system was attached to an upright microscope (Axio Examiner; Zeiss) and the blue light was filtered through a bandpass interference filter (BP 474/28; Zeiss). Using a triple-pass beamsplitter (filter set 62 HE; Zeiss), the light was then directed through a 40× objective (Achroplan, NA 0.75) onto the array-mounted retina, passing through the weighted nylon mesh and hitting the top rod/cone layer first. The blue light stimulus was chosen based on previous work showing that rat ipRGCs are most sensitive to 480 nm light (Berson *et al.* 2002).

MEA voltage recordings were amplified and digitized at 25 kHz using a PC-based A/D interface card and MCRack software (Multi-Channel Systems). The signals were bandpass filtered with cutoffs at 200 Hz and 3 kHz. A detection threshold of –5 standard deviations (SD) from baseline electrical activity was used to identify spike waveforms that were then separated from the continuous data. Clustered spike data were sorted into individual units with Offline Sorter software (Plexon Inc., Dallas, TX, USA). Specifically, spikes that appeared simultaneously on 80% of the channels were removed as noise artifacts, and remaining waveforms were aligned to the global minimum. The waveforms were represented in a 3D feature space and the optimum number of spike clusters was determined using a T-distribution Expectation-Maximization algorithm (degrees of freedom multiplier = 10). The waveforms were then further sorted using an iterative K-means algorithm, with a threshold

of 2 SD used to remove outlier waveforms. Using Neuro-Explorer software (Nex Technologies, Madison, AL, USA), the number of spikes occurring in 1 s bins was counted, and these data were used to generate spike frequency graphs and total counts of the light-evoked spikes. To identify ipRGCs, spike counts were determined for: (1) the 10 s (−10 to 0 s) pre-stimulus period ('x'); (2) the first 10 s (0–10 s) of the light stimulus period ('y'); and (3) the second 10 s (10–20 s) of the light stimulus period ('z'). In the postnatal retinas, identification of 'ipRGC units' was based on all of the following criteria being met: $y \geq 50$, $y \geq 2x$, $z \geq 50$ and $z \geq 2x$. Based on initial visual inspections of the data, these criteria identified units exhibiting robust and prolonged light responses characteristic of ipRGC responses. In the adult retina recordings, the same ipRGC identification criteria were applied to the data obtained in the presence of a synaptic blocker cocktail that silenced rod/cone-driven signalling. Due to the criteria employed, the identified neonatal or adult ipRGC units may have been biased towards selection of M1-type ipRGCs, as the M1 subtype exhibits the most robust light-evoked responses (Schmidt & Kofuji, 2009; Ecker *et al.* 2010). However, while these ipRGC subtypes have been described for mice, it is not currently clear if the same subtypes exist in the rat.

Calcium imaging of ipRGCs isolated by immunopanning

All culture, imaging and immunohistochemistry supplies and solutions were obtained from Sigma-Aldrich unless noted otherwise. For the immunopanning procedure, we used a crude serum containing antibodies raised against rat melanopsin. This serum was collected from rabbits that had been immunized with a peptide (by Open Biosystems, Huntsville, AL, USA) matching the N terminus of rat melanopsin (KMNSPSESRVPSSLTQDPSF, conjugated to KLH carrier protein; sequence from Hattar *et al.* 2002). A portion of the serum was purified against peptide–bovine serum albumin (BSA) affinity columns and titred by indirect enzyme-linked immunosorbent assay (purification by Open Biosystems). The purified antibodies were stored at −80°C in 50% glycerol aliquots and used for immunohistochemical staining of rat retinal sections to verify antibody effectiveness. Posterior eyecups were dissected from adult Long Evans rats, rinsed with 0.1 M PBS, and fixed in 4% paraformaldehyde/PBS for 1 h. After rinsing with 0.1 M PBS three times, the tissue was embedded in a 20% sucrose/PBS cryoprotection solution overnight at 4°C. The following day, the eyecups were embedded in optimal cutting temperature (OCT) compound (Tissue-Tek, Torrance, CA, USA) and cut into 20 μm slices using a cryostat. Sections were slide-mounted and stored at −80°C until use. Prior to use, slides were defrosted and washed with 0.1 M PBS before being blocked for 1 h with a PBS solution containing 10% normal goat serum (Life Technologies), 2% BSA and 0.3% Triton X-100. The primary anti-melanopsin antibodies were diluted (1:2000) in an incubation PBS-based buffer containing 1% BSA, 1% normal goat serum, 0.3% Triton X and 0.01% sodium azide, and the retinal sections were covered in this solution overnight at 4°C. Sections were washed three times with 0.1 M PBS for 15 min before being incubated for 1 h at room temperature in buffer diluted (1:1000) with goat anti-rabbit secondary antibody conjugated to Alexa Fluor 594 dye (Life Technologies). After incubation, the sections were rinsed in 0.1 M PBS three times for 15 min and coverslipped in Flourmount (SouthernBiotech, Birmingham, AL, USA). Immuno-labelled retinal sections were visualized using an inverted light microscope (Axio Examiner; Zeiss) equipped with a mercury-based light source.

Purified ipRGC cultures were prepared from litters of 5- to 6-day-old Long Evans rats (6–8 per session), killed by isoflourane overexposure and decapitation, using an anti-melanopsin plate adhesion immunopanning technique that has been previously described (Hartwick *et al.* 2007). In brief, retinas were dissected in Hibernate-A medium (Brain Bits) supplemented with B-27 (Life Technologies) and gentamicin. The retinas were incubated for 30 min in Ca^{2+}/Mg^{2+}-free Dulbecco's phosphate buffered solution (DPBS; Life Technologies) containing papain (Worthington Biochemicals, Lakewood, NJ, USA), L-cysteine and DNase. The retinas were then mechanically triturated and washed in Ca^{2+}/Mg^{2+}-containing DPBS enzyme inhibitor solutions containing DNase and sequentially increasing concentrations of ovomucoid (Roche Diagnostics, Indianapolis, IN, USA) and BSA. The cells were resuspended in DPBS with added insulin and BSA, and incubated on dishes that had been pre-coated with lectin (*Griffonia* [*Bandeiraea*] *simplicifolia* lectin I; Vector Laboratories, Burlingame, CA, USA) to aid in elimination of non-specific binding of contaminating cell types, such as macrophages and microglia.

The remaining cell suspension was incubated on a Petri dish that had been coated first with goat anti-rabbit IgG antibodies (Jackson ImmunoResearch, West Grove, PA, USA), and then with rabbit anti-rat melanopsin anti-bodies (in crude serum; described above). After this incubation, non-adherent cells were discarded by rinsing the dish with DPBS. Adherent cells were exposed to a 0.125% trypsin solution (8 min at 37°C) and then released by pipetting an enzyme-inhibiting solution (30% fetal bovine serum in NbActiv4 medium; BrainBits) along the dish. The isolated immunopanned cells were plated on 12 mm poly-D-lysine (PDL)/laminin-coated coverslips in NbActiv4 supplemented with 40 ng ml^{-1} brain-derived neurotrophic factor (BDNF), 10 ng ml^{-1} ciliary neuro-trophic factor (CNTF), 10 μM forskolin and 10 mg ml^{-1}

gentamicin, and they were maintained in an incubator at 37°C in the dark, under a 5% CO_2–air environment.

Calcium imaging methodology was modified from previous work (Hartwick *et al.* 2007). After 1–2 days in culture, coverslip-plated ipRGCs were loaded with 10 μM Fura-2 AM calcium indicator dye (Life Technologies) that had been solubilized in Hank's balanced salt solution (HBSS; with 10 mM Hepes, pH 7.4) containing 0.1% pluronic F-127 (Life Technologies). After 30 min in the dark at 37°C, the fura-loaded cells were placed in a chamber (Bioptechs, Butler, PA, USA) on the stage of the Axio Examiner microscope (Zeiss) that was constantly superfused with heated (32–34°C), oxygenated HBSS (10 mM Hepes, pH 7.4). Individual cells were located using a dim white microscope light, which aided in the identification of light-responding cells (i.e. cells that exhibited elevated calcium levels due to this light that then recovered in the dark). These cells were then maintained in the dark for at least 15 min before being stimulated with 20 s pulses of the same blue LED light (470 nm; Colibri, Zeiss) described above for the MEA experiments.

Images of fluorescence (510 nm emission) were captured using a 20× objective (Plan-Apochromat, NA 1.0; Zeiss) and a cooled charged-coupled device camera (Sensicam; Cooke, Romulus, MI, USA) attached to the microscope. The two excitation lights were generated by 365 and 380 nm LED modules in the Colibri illumination system, and both lights were further filtered through 360 and 380 nm (FF01-380/14, FF01-360/12; Semrock, Lake Forest, IL, USA) narrow-band filters, respectively. A custom dichroic beam-splitter (365DCLP; Chroma Technology, Rockingham, VT, USA) separated the two LED modules within the Colibri casing, and the two excitation lights then passed through a triple-pass beamsplitter (filter set 62 HE; Zeiss) in the microscope before being directed through the objective. Using Imaging Workbench 6.0 software (Indec Biosystems, Santa Clara, CA, USA), the fluorescence intensity in individual ipRGC somata was captured and quantified for ratiometric calcium imaging. The narrow-band 360 nm light (currently the lowest wavelength available for the Colibri system) is close to the isosbestic point of fura-2. Thus, as the intracellular free Ca^{2+} increased, the fura-2 (360/380 nm) ratio increased due to: (1) a decrease in fluorescence with 380 nm excitation; and (2) unchanged fluorescence with 360 nm excitation (or a smaller decrease relative to 380 nm).

Fura-2 ratios were obtained every 5 s during light stimuli and every 10–40 s during the intervening dark periods. Light responsive cells were defined as those exhibiting a greater than 15% rise in fura-2 ratio from baseline. The Δfura-2 ratio was calculated as peak minus baseline fura-2 ratio. Baseline was determined by averaging the fura-2 ratio of the three ratios preceding each 20 s light pulse while the peak was defined as the maximum fura-2 ratio observed within the first 60 s following light onset.

Pharmacology and solution preparation

Stock solutions were prepared, aliquoted and stored at −80°C, with non-water soluble compounds being dissolved in dimethyl sulfoxide (DMSO). The final working concentration of DMSO in the Ames medium or HBSS was ≤0.1%. Unless stated otherwise, each compound was perfused onto the retinas for 5 min prior to light stimulation.

To investigate cAMP/protein kinase A (PKA) signalling pathways, forskolin was obtained from Sigma-Aldrich; 8-bromoadenosine-3′,5′-cyclic monophosphate sodium salt (8-Br-cAMP), 8-bromoguanosine cyclic 3′,5′-monophosphate sodium salt (8-Br-cGMP), ($\pm$)-*N*-[(1*R**,2*R**)-2-phenylcyclopentyl]-azacyclotridec-1-en-2-amine hydrochloride (MDL 12330A) and protein kinase inhibitor-(14–22)-amide, myristoylated (PKI 14–22 amide) were obtained from Tocris Bioscience (Minneapolis, MN, USA); 5, 6-dichloro-1-β-D-ribofuranosylbenezimidazole-3′, 5′-cyclic monophosphorothioate, Sp-isomer (Sp-5,6-DCl-cBIMPS) and 8-(4-chlorophenylthio) guanosine-3′, 5′-cyclic monophosphate (8-pCPT-cGMP) were obtained from Biolog (Bremen, Germany). To investigate adenosine-mediated signalling pathways, adenosine, N^6-cyclopentyladenosine (CPA), 1-[2-chloro-6-[[(3-iodophenyl)methy l]amino]-9*H*-purin-9-yl]-1-deoxy-*N*-methyl-β-D-ribofu ranuronamide (Cl-MECA), 6-*S*-[(4-nitrophenyl)methyl]-6-thioinosine (NMBPR) and 8-cyclopentyl-1,3-dipropylxanthine (DPCPX) were all obtained from Tocris Bioscience.

Melanopsin-based light responses were isolated in the intact adult retinas by superfusing a cocktail of synaptic blockers onto the retinas to inhibit rod/cone-driven signalling (Wong *et al.* 2007). Glutamatergic signalling was inhibited using 100 μM metabotropic glutamate receptor agonist L-(+)-2-amino-4-phosphonobutyric acid (L-AP4; Tocris) and 25 μM AMPA receptor antagonist 2,3-dioxo-6-nitro- 1,2,3,4- tetrahydrobenzo[*f*] quinoxali ne-7-sulfonamide (NBQX; Tocris). The NMDA-type glutamate receptor antagonist MK-801 (10 μM) was also added to the cocktail for adult experiments involving adenosinergic agents (adenosine, NMBPR, CPA, Cl-MECA and DPCPX). Cholinergic signalling was inhibited using 10 μM muscarinic receptor antagonist atropine (Sigma-Aldrich) and 100 μM nicotinic receptor antagonist tubocurarine (Tocris). GABA$_A$, GABA$_B$ and GABA$_C$ receptors were blocked with 50 μM picrotoxin (Tocris), 5 μM 3-[[(3,4-dichlorophenyl)methyl]amino]propyl] diethoxymethyl)phosphinic acid (CGP 54626; Tocris), and 100 μM (1,2,5,6-tetrahydropyridin-4-yl)methylphosphinic acid (TPMPA;

Sigma-Aldrich), respectively. Glycinergic signalling was inhibited by 10 μM strychnine (Tocris). Light responses recorded in the adult retinas in the presence of Ames medium containing this blocker cocktail were deemed to be the melanopsin-dependent responses of ipRGCs.

Data analysis

Preparation of final graphs and statistical comparisons were performed using Sigmaplot 12 software (Systat Software, San Jose, CA, USA). The overall light-evoked spike counts were quantified by adding the number of spikes that occurred during the 20 s light pulses with those that occurred during the initial 80 s post-stimulus for each unit. All data are expressed as the mean $\pm$ standard error of the mean (SEM). Due to the higher number of light-sensitive units in the neonatal retinas, multiple units were often recorded on a single electrode. The number of units identified by the spike sorting software in each postnatal retina was not always identical across different treatment conditions (i.e. before, during and after drug treatment). The number of units (n) reported in the Results therefore represented the total number of units identified in the 'drug present' condition. Statistical differences in the spike counts obtained from the post-natal retinal recordings were determined using one-way analysis of variance (ANOVA) and Holm–Sidak *post hoc* testing. In the adult retinas, there were fewer (usually < 4) light-sensitive units recorded from each retina, allowing responses from individual cells to be matched across the different conditions (before, during and after drug treatment). Statistical differences in the spike counts obtained from the adult retina recordings were therefore determined using one-way repeated-measures ANOVA and Holm–Sidak *post hoc* testing.

Results

Modulation of ipRGC light responses through a cAMP-mediated pathway

While melanopsin-dependent light responses in rodent ipRGCs are present from birth, rod- and cone-driven light responses in ganglion cells do not occur until later in development (Hannibal & Fahrenkrug, 2004; Sekaran *et al.* 2005; Tu *et al.* 2005). This enables the neonatal rodent retina to serve as a useful preparation for studying ipRGC photoresponses in the absence of rod/cone-influenced signalling pathways. Using MEA recordings from the ganglion cell layer, we recorded light-evoked action potential firing from postnatal (P) retinas of Long-Evans rats (example from P8 retina in Fig. 1A). These responses persisted in the presence of a cocktail of glutamate, acetylcholine, GABA and

glycine receptor antagonists (see Methods for details), thereby confirming that the light responses reflected the inherent melanopsin-related responses of ipRGCs (Fig. 1B). In the absence of synaptic blocker cocktail, we observed the emergence of rod/cone-driven responses (characteristics discussed in next section; see Fig. 4) to coincide closely with eye opening, which usually occurred at P15 in the Long-Evans rats. In this study, all MEA retinal recordings denoted as 'neonatal ipRGCs' were obtained from rats during their second week of life (age P8–P14).

Prior to eye opening, spontaneous waves of correlated activity sweep across the retina and these waves are essential for proper development and refinement of retinal circuitry. During the second week of life in rodents, the neurotransmitter that drives retinal waves switches from acetylcholine (Stage II) to glutamate (Stage III) (Ford & Feller, 2012). In addition to this excitatory input, ganglion cells also receive GABA- and glycine-mediated inhibitory input during the waves (Blankenship *et al.* 2009). Thus, the synaptic blocker cocktail was designed to block all excitatory and inhibitory drive to the ganglion cells and, as expected, the waves of activity were silenced in post-natal retinas during superfusion of the cocktail. Although the peak firing frequency of ipRGCs was not significantly affected, the mean duration of ipRGC responses to the 20 s bright (7.1×10^{15} photons s^{-1} cm^{-2}) blue light stimulus was shortened after exposure to the cocktail for 5 min (compare Fig. 1B to 1A). In quantifying this effect, the recovery of mean spike frequency to a near baseline rate of 2 spike s^{-1} occurred 25 s earlier (37 s *versus* 62 s post-light onset) with the blocker cocktail present compared to when it was absent (Fig. 1C).

As the membrane depolarization associated with the spontaneous waves of activity are known to induce elevations in intracellular cAMP in retinal neurons (Meyer-Franke *et al.* 1995; Dunn *et al.* 2006), we hypothesized that the shortened ipRGC responses were due, at least in part, to reductions in intracellular cAMP caused by the silencing of spontaneous activity. To test this hypothesis, we investigated the effect of forskolin on neonatal ipRGC responses to 20 s blue light exposure in the presence (Fig. 2A) and absence (Fig. 2B) of the synaptic blocker cocktail. Forskolin has been shown to induce cAMP elevations in retinal neurons (Dunn *et al.* 2006). The light irradiance (3.9×10^{15} photons s^{-1} cm^{-2}) was reduced from that used in Fig. 1 to prevent response saturation or depolarization block from potentially masking forskolin's effects, and this light stimulus was used for all subsequent experiments. With the cocktail absent, waves of activity persisted and light pulses were timed to occur after a wave passed through the recorded retinal region, as the average inter-wave interval is longer than 60 s at later (stage III) postnatal ages (Blankenship *et al.* 2009). In this blocker-free condition, the recovery
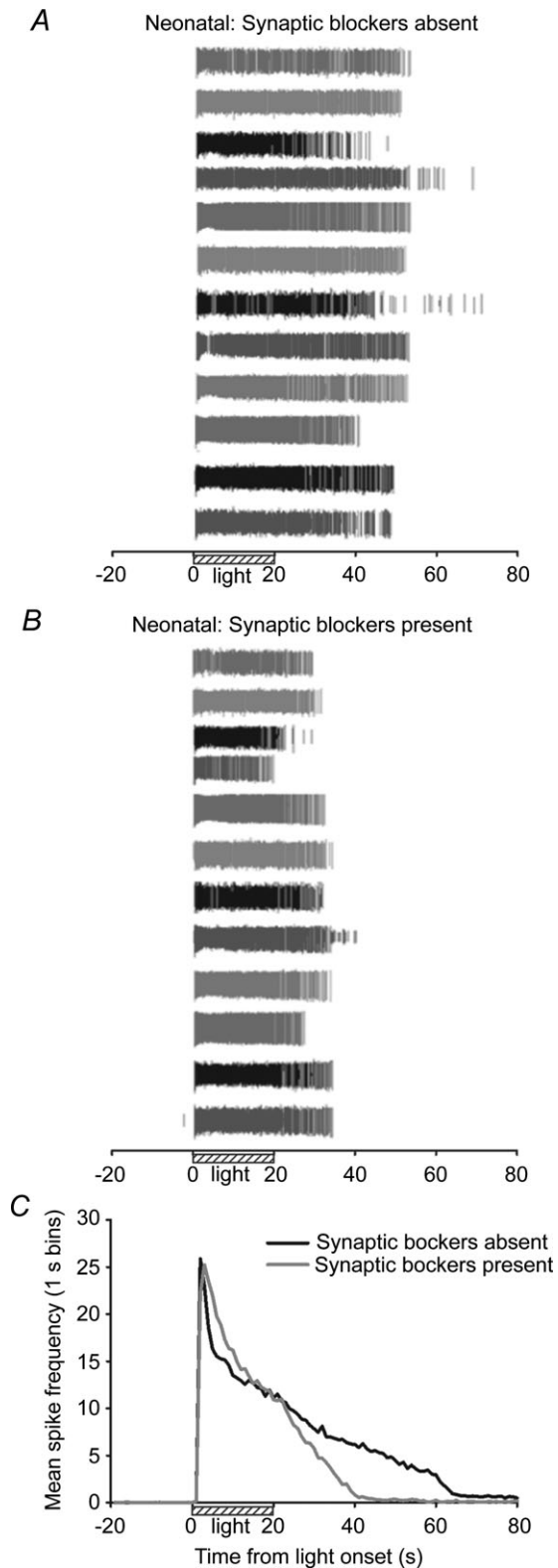
of mean spike frequency to a rate of 2 spikes s^{-1} took 24 s longer (based on 1 s binning of spike counts) after exposure to 10 μM forskolin for 5 min, relative to the pre-treatment response (Fig. 2*C*). Total counts of light-evoked spiking were quantified by adding together the number of spikes that occurred during the 20 s light exposure plus 60 s post-stimulus period. With lengthening of the response duration, the mean light-evoked spike count was also significantly higher during forskolin treatment, as compared to both the pre- ('control') and post-treatment ('washout') conditions (Fig. 2*D*). Similarly, forskolin significantly increased ($P < 0.001$; *t* test) mean ipRGC spike counts with synaptic blockers present ($N = 3$ retinas; $n = 60$ cells; data not shown graphically but example in Fig. 2*A*), indicating that forskolin's effect was not due to increased release of the major excitatory and inhibitory neurotransmitters.

Forskolin directly stimulates the cAMP-generating enzyme adenylate cyclase without interacting with cell-surface receptors (Seamon *et al.* 1981). Changes in internal cAMP can regulate a number of intracellular signalling pathways, including the actions of the phosphorylating enzyme PKA, which requires cAMP for its activation. However, forskolin can also affect cells through cAMP-independent mechanisms (Laurenza *et al.* 1989). To demonstrate that the effect of forskolin on ipRGC light responses involved a cAMP-dependent signalling pathway, we assessed whether blockade of either adenylate cyclase or PKA altered the effect of forskolin. In the presence of 50 μM MDL 12330A, a widely used specific inhibitor of adenylate cyclase (Seifert *et al.* 2012), the response lengthening effect of the 10 μM forskolin treatment was abolished (Fig. 2*E*, *G*). The actions of forskolin were similarly blocked when retinas were treated with the cell-permeable version of PKI-(14–22)-amide (10 μM; Fig. 2*F*, *G*), a compound that renders PKA inactive by specifically binding to this enzyme's endogenous catalytic sites (Murray, 2008), thereby demonstrating that PKA is a downstream component of the forskolin-initiated signalling cascade.

We next tested whether cyclic nucleotide analogues and protein kinase agonists could mimic the effects of forskolin. Superfusion of neonatal retinas with the cell-permeable cAMP analogue 8-Br-cAMP (1 mM) for 5 min significantly increased the total number of light-evoked spikes fired by ipRGCs (Fig. 3*A*, *C*). To control for any non-specific effects of the brominated

Figure 1. Effect of spontaneous activity blockade on neonatal ipRGC light responses
A and *B*, extracellular MEA recordings of light-evoked spikes from 12 ganglion cells from a P8 rat retina before (*A*) and during (*B*) treatment with a cocktail of glutamate, acetylcholine, GABA and glycine antagonists. Different shading of spike trains facilitates matching of individual cells in the two conditions. *C*, mean spike frequency (spikes per 1 s bins) recorded before, during and after light stimulation ($N = 3$ retinas; $n = 70$ cells). The ipRGC responses to 20 s blue light (470 nm; 7.1×10^{15} photons s^{-1} cm^{-2}) shortened in duration following 5 min exposure to synaptic blocker cocktail.
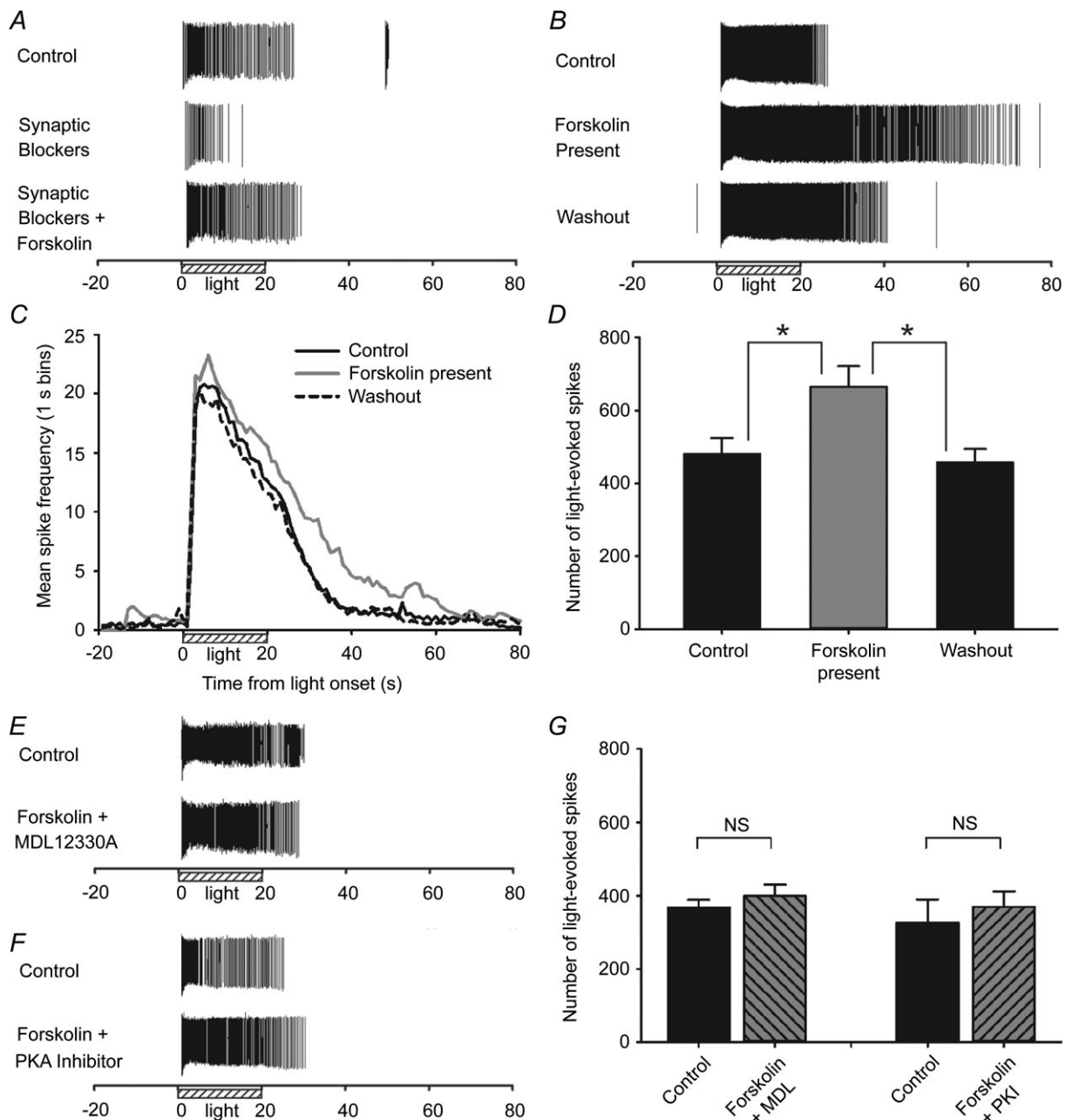
Figure 2. Effect of forskolin, an adenylate cyclase stimulator, on neonatal ipRGC light responses
A, example light response recordings from a cell before and during 5 min treatment with 10 μM forskolin, in the presence of the synaptic blocker cocktail; *B*, from another cell with the blocker cocktail absent. 'Control' responses were recorded from retinas superfused with Ames medium alone. *C* and *D*, summary of mean spike frequency (*C*, spikes s^{-1}) and mean overall spike counts (*D*) from light-stimulated ipRGCs ($N = 3$, $n = 67$), recorded in the absence of the blocker cocktail. *$P < 0.05$, one-way ANOVA, *post hoc* Holm–Sidak test. *E* and *F*, example light responses recorded from ipRGCs before and during the 5 min exposure to 10 μM forskolin plus (*E*) adenylate cyclase inhibitor MDL 12330A (MDL; 50 μM) or (*F*) PKA inhibitor PKI-(14–22)-amide (10 μM). *G*, mean spike counts show that both MDL ($N = 3$; $n = 64$) and PKI ($N = 2$; $n = 19$) blocked the effect of forskolin on ipRGC light responses. NS, not significant ($P > 0.05$, one-way ANOVA). Stimulus was blue light (470 nm; 3.9×10^{15} photons s^{-1} cm^{-2}).

compound, retinas were also treated with the cGMP analogue 8-Br-cGMP (1 mM) and no discernible effects on ipRGC responses were observed (Fig. 3B, C). Similar to 8-Br-cAMP, bath application of the potent PKA activator Sp-5,6-DCl-cBIMPS (cBIMPS; 100 μM) increased ipRGC spiking elicited by light stimulation (Fig. 3D, F). The continued lengthening of ipRGC light responses after drug washout can probably be attributed to the fact that this compound, unlike 8-Br-cAMP, is resistant to degradation by phosphodiesterases (Murray,

2008). Conversely, stimulation of the cGMP-dependent kinase, protein kinase G (PKG), with 8-pCPT-cGMP (100 μM) did not significantly affect light-evoked firing (Fig. 3E, F), either during drug application or 20 min after washout. Taken together, the results shown in Figs 2 and 3 provide strong evidence that stimulation of the signalling cascade involving adenylate cyclase, cAMP and PKA results in an increase in the number and duration of light-evoked spikes fired by neonatal ipRGCs.
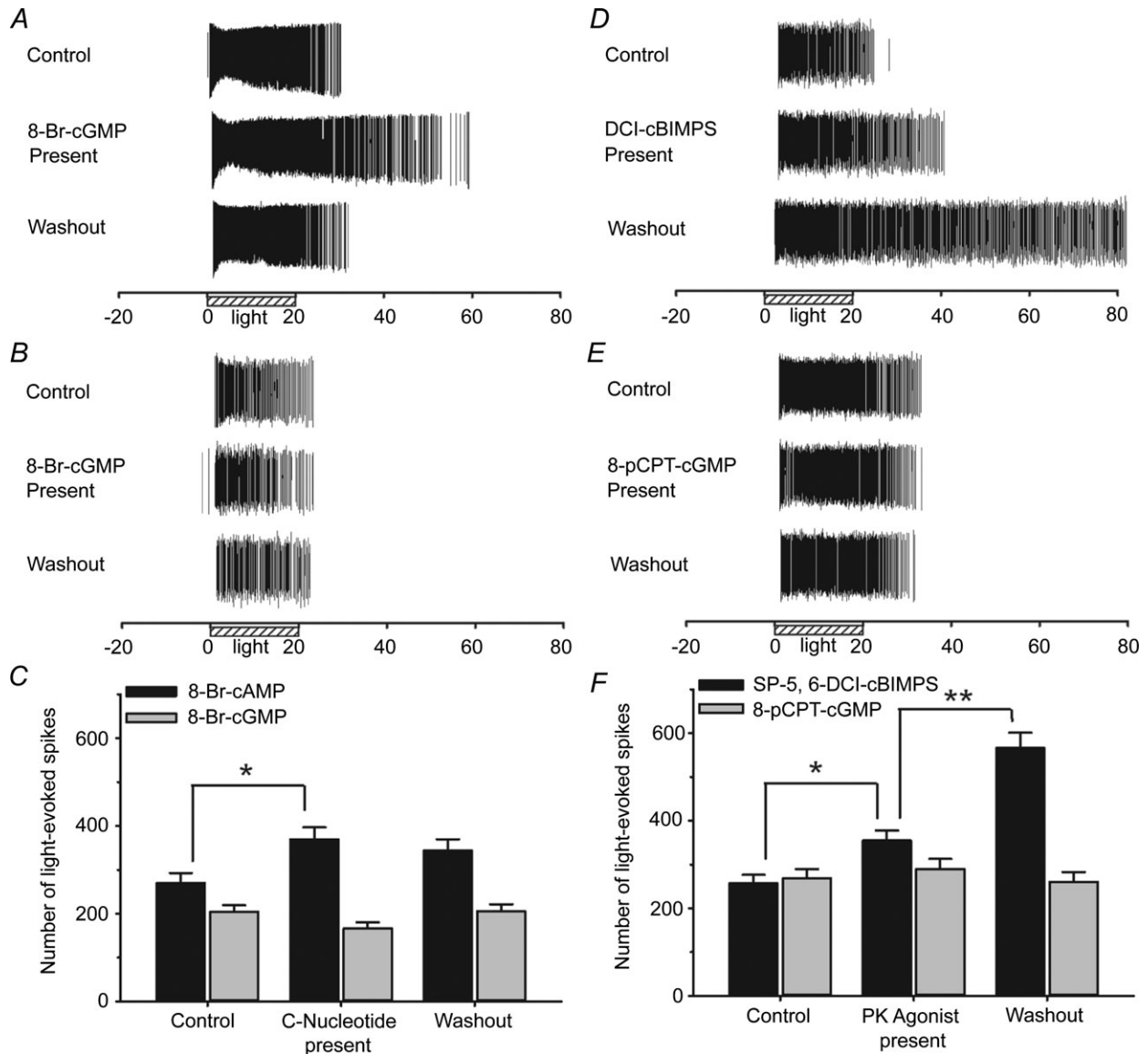

Figure 3. Role for cAMP and PKA in modifying neonatal ipRGC light responses
A and B, example spike rasters from a light-stimulated ipRGC before, during and after 5 min exposure to the cyclic nucleotide analogues (A) 8-Br-cAMP (1 mM) or (B) 8-Br-cGMP (1 mM). C, mean spike counts showing that the cAMP analogue ($N = 3$; $n = 35$), but not the cGMP analogue ($N = 4$; $n = 54$), significantly increased ipRGC spiking. D and E, similarly, the non-hydrolysable PKA agonist Sp-5,6-DCl-cBIMPS (D; $N = 3$; $n = 38$) significantly affected ipRGC light responses, while the PKG agonist 8-pCPT-cGMP (E; $N = 3$; $n = 47$) did not. F, mean spike count data illustrating effects of the 5 min treatments with the protein kinase agonists. $**P < 0.01$, $*P < 0.05$, one-way ANOVA, Holm–Sidak. Stimulus was blue light (470 nm; 3.9×10^{15} photons s^{-1} cm^{-2}).
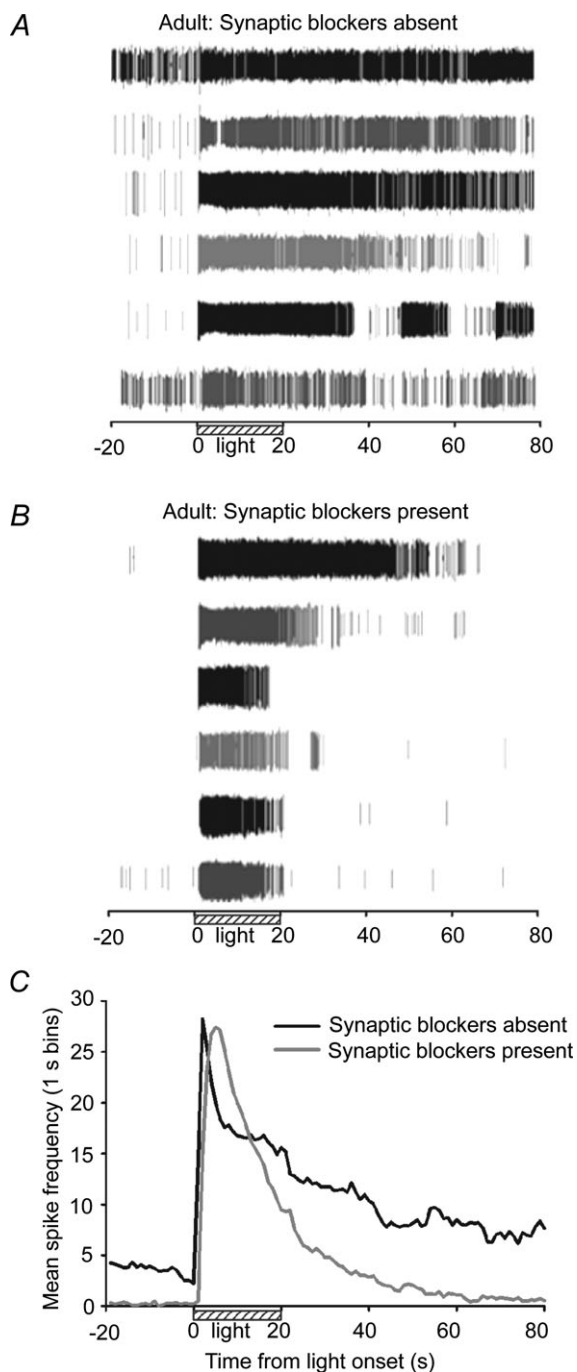
Figure 4. Effect of synaptic activity blockade on adult ipRGC light responses

A and *B*, spike rasters from six ipRGCs recorded from three adult (>2 months old) rat retinas before (*A*) and during (*B*) treatment with cocktail of glutamate, acetylcholine, GABA and glycine antagonists that blocked synaptically driven activity. *C*, mean spike frequency (1 s binning) recorded over time in the light-stimulated retinas (*N* = 10 retinas; *n* = 35 cells). In addition to eliminating the rod/cone-driven spiking, evident by the absence of the short-latency initial burst in spiking, perfusion with synaptic blocker cocktail shortened the duration of ipRGC responses to 20 s blue light (470 nm; 3.9×10^{15} photons s^{-1} cm^{-2}).

The wave-dependent elevations of cAMP that occur in postnatal RGCs play a critical role in the refinement of the connections between these retinal output neurons and their appropriate brain targets (Stellwagen & Shatz, 2002). We next sought to determine whether the cAMP-mediated effect on ipRGC light responses was solely a developmental phenomenon or if it remained after retinal circuit wiring was completed. After eye opening in the Long-Evans rats, which occurred at approximately P15, faster and more transient light responses could be recorded from the ganglion cell layer, consistent with expected rod/cone-driven signalling. The inherent responses of ipRGCs were identified based on the persistence of light-evoked spiking in the presence of synaptic blocker cocktail (see Methods for details). During superfusion of the synaptic blocker cocktail, the units that only exhibited transient (<5 s) responses to the 20 s light pulses prior to cocktail application (presumed non-photosensitive RGCs receiving rod/cone-driven signals) were eliminated from the recordings. In addition to their melanopsin-based photosensitivity, ipRGCs also receive synaptic input from bipolar and amacrine cells (Belenky *et al.* 2003; Wong *et al.* 2007), and the rod/cone-driven component was evident by comparing the difference in spiking during the first couple of seconds of the light responses recorded from the older (age > 2 months) rat retinas before and after application of the synaptic blocker cocktail (Fig. 4). Light responses from subsequently identified ipRGCs, recorded pre-cocktail application, exhibited an abrupt burst in spiking with short latency from light onset (Fig. 4*C*). This is consistent with the initial component of adult ipRGC light responses, recorded in the absence of synaptic blockers, being rod/cone-driven. Although ipRGC light responses persisted for many seconds after light onset with cocktail present, the responses from these same cells were even more prolonged in the pre-treatment recordings (compare Figs 4*A* and 4*B*; data summary in Fig. 4*C*). When the synaptic connections between these cells and other retinal neurons were not inhibited, there was more background spiking activity evident in the dark (Fig. 4*A*, *C*), suggesting that the spontaneous activity present in the older retinas promotes lengthening of ipRGC light responses in a similar fashion to how wave-mediated activity influenced the neonatal ipRGC light responses (Fig. 1).

In the presence of synaptic blocker cocktail (to identify light-responding ipRGCs), we treated the older retinas for 5 min to either 10 μM forskolin (Fig. 5*A*, *B*) or 1 mM 8-Br-cAMP (Fig. 5*C*, *D*). Similar to the neonatal retinal experiments (Figs 2 and 3), both compounds significantly increased the total number of spikes fired during and after (20 s light exposure plus 60 s post-illumination period) light stimulation. Thus, the effect of cAMP on ipRGC light responses is not restricted to early development, and is instead a fundamental feature of rat melanopsin-based ipRGC photoresponses.

Modulation of ipRGC light responses through A_1 adenosine receptor activation

Adenosine is a known neuromodulator present in the inner retina (Hartwick *et al.* 2004) that influences intracellular cAMP levels by either stimulating or inhibiting adenylate cyclase. We therefore tested the effect of adenosine on MEA-recorded ipRGC spiking, seeking to determine whether this endogenously present compound modifies ipRGC light responses through the cAMP-mediated pathway outlined above. Adenosine (500 μM) was bath applied to neonatal (P8–14) rat retinas in the presence of adenosine transport inhibitor NMBPR (20 μM) (Fig. 6A). After 5 min exposure to these two compounds, the duration of the ipRGC responses was considerably shortened (Fig. 6B), with significantly fewer light-evoked spikes fired (Fig. 6C). As the effect of the adenosine treatment was most consistent with a reduction in cAMP levels (i.e. opposite effect as occurred with forskolin treatment), we investigated whether adenosine's effect is mediated through A_1 receptors. These adenosine receptors are linked to G_i-mediated

inhibition of adenylate cyclase (Fredholm *et al.* 2001). After treatment with adenosine plus NMBPR (20 min later), the retinas were exposed to these compounds again with the A_1 receptor antagonist DPCPX (20 μM) present in the bath. This antagonist blocked the effect of adenosine, with responses recorded during the bath application of all three agents together (adenosine, NMBPR and DPCPX) being no different from the initial control light responses recorded in Ames medium alone (Fig. 6A–C). Confirming the involvement of A_1 adenosine receptors, exposure of neonatal retinas to the specific agonist CPA (10 μM) produced a similar effect as adenosine + NMBPR in reducing the duration of light-evoked ipRGC spiking (Fig. 6D–F). A_3 receptors have also been linked to G_i protein-mediated inhibition of adenylate cyclase and have been found on mammalian ganglion cells (Zhang *et al.* 2006), but the selective A_3 agonist 2-Cl-IB-MECA (10 μM) did not significantly ($P > 0.05$, one-way repeated-measures ANOVA; compared to control and washout conditions) affect the number of light-evoked spikes fired by the ipRGCs in the neonatal retinas ($N = 3$ retinas, $n = 107$ cells; data not shown).
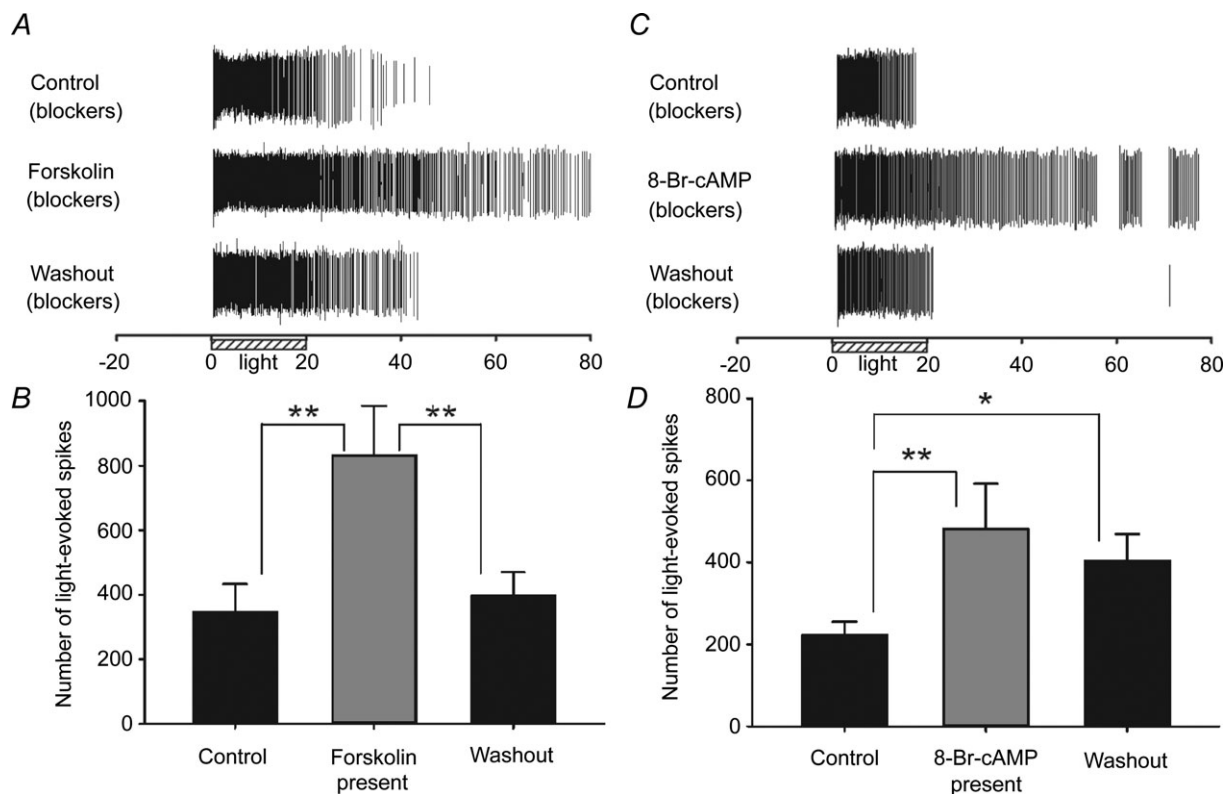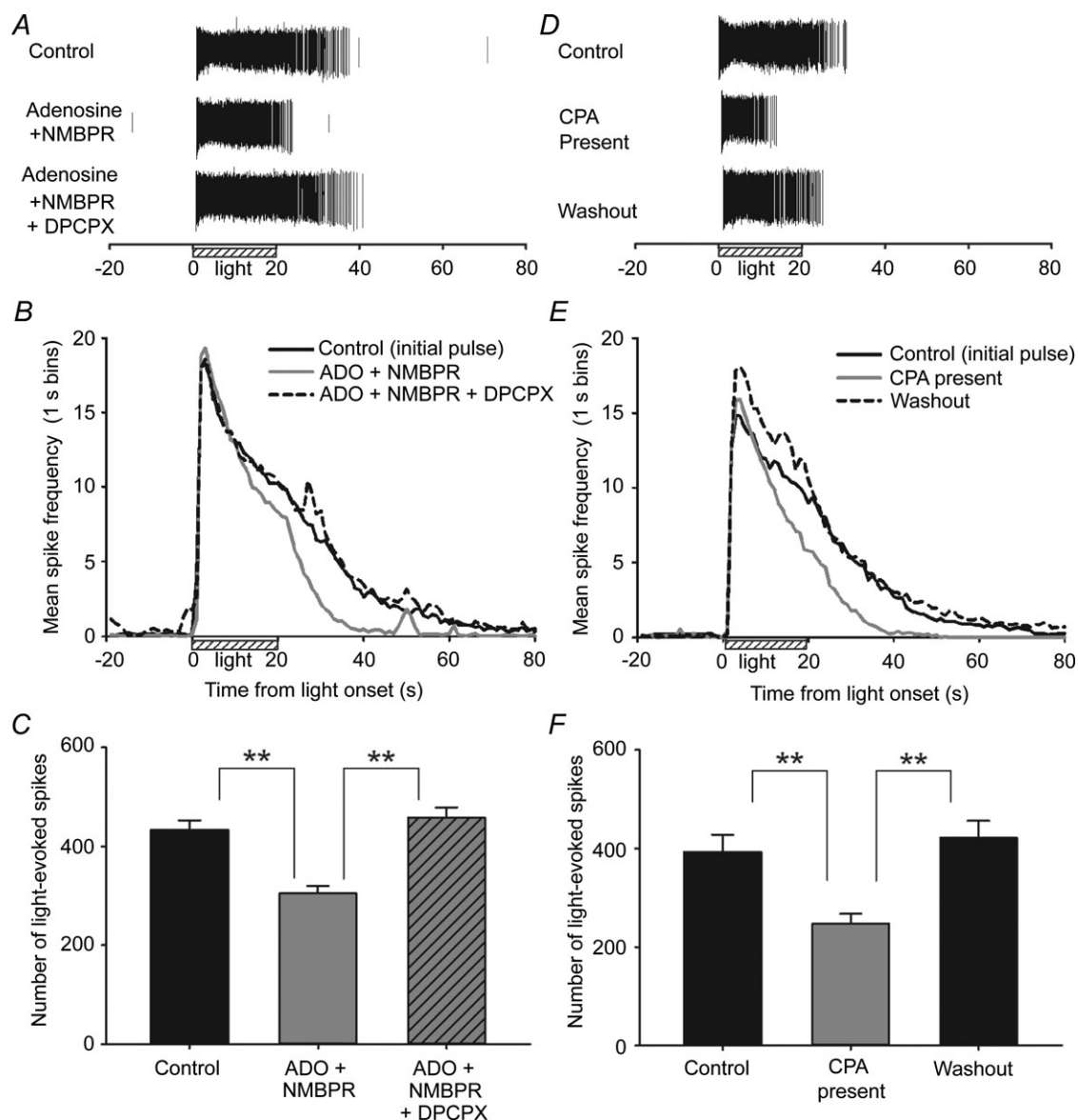

Figure 5. Role for cAMP in modifying adult ipRGC light responses
A and *B*, example spike rasters (*A*) and mean spike count data (*B*) for light-stimulated ipRGCs ($N = 3$; $n = 14$) recorded from adult (>2 months old) rat retinas before, during and after 5 min treatment with 10 μM forskolin. *C* and *D*, similarly, example rasters (*C*) and mean spike count data (*D*) for adult ipRGCs ($N = 3$; $n = 9$) treated with 1 mM 8-Br-cAMP for 5 min. **P < 0.01, *P < 0.05, one-way repeated-measures ANOVA, Holm–Sidak. All light responses (control, drug treatment, washout) in these data were recorded in the presence of synaptic blocker cocktail to confirm recordings were from ipRGCs. Stimulus was blue light (470 nm; 3.9 × 10^{15} photons s^{-1} cm^{-2}).

To investigate whether the effect of adenosine on neonatal ipRGC light responses was mediated through a decrease in internal cAMP levels, we next assessed whether the pharmacological elevation of cAMP could reverse the shortening effect CPA had on the duration of light-evoked ipRGC spiking. Exposure for 5 min to CPA (10 μM) alone significantly decreased the duration of ipRGC light responses (Fig. 7A–C), consistent with previous experiments (Fig. 6D–F). Before the

next light exposure, CPA was washed from the bath and the retinas were constantly superfused with 1 mM 8-Br-cAMP for 20 min, with 10 μM CPA being added to the superfusing medium for the last 5 min. The duration of the responses and total number of light-evoked spikes fired by the ipRGCs was significantly increased after this CPA plus 8-Br-cAMP pre-treatment as compared to application of CPA alone (Fig. 7A–C).

Figure 6. Adenosine A$_1$ receptor-mediated modulation of neonatal ipRGC light responses
A, example rasters from an ipRGC treated for 5 min with 500 μM adenosine (ADO) + 20 μM NMBPR (ADO transport inhibitor) in the absence and presence of 20 μM DPCPX (A$_1$ receptor antagonist). B and C, summary graphs of mean spike frequency (B; 1 s binning) and mean spike counts for these experiments (C; N = 3; n = 97). D–F, Similar to ADO treatment, a 5 min treatment with A$_1$-receptor agonist CPA (D; 10 μM) shortened light responses (E) and reduced the total number of light-evoked spiking in neonatal ipRGCs (F); N = 3; n = 39). **P < 0.01, *P < 0.05, one-way ANOVA, Holm–Sidak. Stimulus was blue light (470 nm; 3.9 × 10^{15} photons s^{-1} cm^{-2}).

In determining whether the effects of adenosine were a unique feature of developing retinas, we tested whether A_1 receptor activation could alter the light responses recorded from ipRGCs in adult (>2 month old) rats. As before, these experiments were done in the presence of bath-applied synaptic blocker cocktail to identify light-responding ipRGCs. Similar to the results obtained using neonatal retinas, 500 μM adenosine (with 20 μM NMBPR) decreased the total number of spikes fired by

Figure 7. Effects of adenosine on neonatal ipRGC light responses can be reversed by cAMP application
Example raster (*A*), mean spike frequency (*B*) and mean spike counts (*C*) for light-stimulated ipRGCs (*N* = 3; *n* = 83) treated for 5 min with 10 μM CPA alone and in co-treatment with 1 mM 8-Br-cAMP. For the last named, the cells were perfused with 8-Br-cAMP for 15 min before the 5 min co-treatment. 'Control' responses were the initial pretreatment responses recorded with only Ames medium in the bath. **$P < 0.01$ ANOVA, Holm–Sidak. Stimulus was blue light (470 nm; 3.9×10^{15} photons s^{-1} cm^{-2}).

the light-stimulated ipRGCs and this effect was blocked by the A_1 antagonist DPCPX (20 μM; Fig. 8*A*, *B*). Furthermore, bath application of the A_1 receptor agonist CPA (10 μM) for 5 min significantly reduced light-driven ipRGC spiking, and this inhibitory effect persisted after the 20 min washout period (Fig. 8*C*, *D*). These results provide physiological evidence that the effect of adenosine on adult ipRGCs is mediated through A_1 receptor activation.

As the MEA experiments reported above involved bathing the flat-mounted retinas with the tested compounds, we considered the possibility that adenosine may be acting on other retinal cells, and adenosine's effect on ipRGCs was an indirect one due to the release of different transmitters/modulators from these adenosine-stimulated cells. The experiments on the adult retinas were done in the presence of synaptic blockers (glutamate, GABA, glycine, acetylcholine receptor antagonists), thereby reducing, but not eliminating, the likelihood of this possibility. To confirm that our observed effects are due the direct effect of adenosine on A_1 receptors present on ipRGCs, we used fura-2 calcium imaging on ipRGCs from near-purified cultures that had been generated through an immunopanning technique that we have used previously (Hartwick *et al.* 2007). For this technique, we used antibodies targeted against the extracellular N terminus of the melanopsin photopigment (Fig. 9*A*). The cells maintain their light sensitivity for the first 2–3 days in culture, which was measured as light-evoked calcium influx using fura-2 calcium imaging techniques (Fig. 9*B*). The calcium signal directly correlates to ipRGC spiking, as the influx is predominantly due to the opening of voltage-gated calcium channels that occurs after action potential firing (Hartwick *et al.* 2007). Adenosine (100 μM) significantly reduced the light-evoked calcium signals, which were measured as an increase in the fura-2 ratio (Fig. 9*C*, *D*). The effect of adenosine was abolished when the isolated cells were pre- and co-treated with the A_1 adenosine receptor antagonist DPCPX (10 μM; Fig. 9*C*, *E*). As the effects of adenosine on ipRGC light responses were preserved in these purified cultures, these results confirm that adenosine acts directly on A_1 adenosine receptors expressed by the rat ipRGCs themselves.
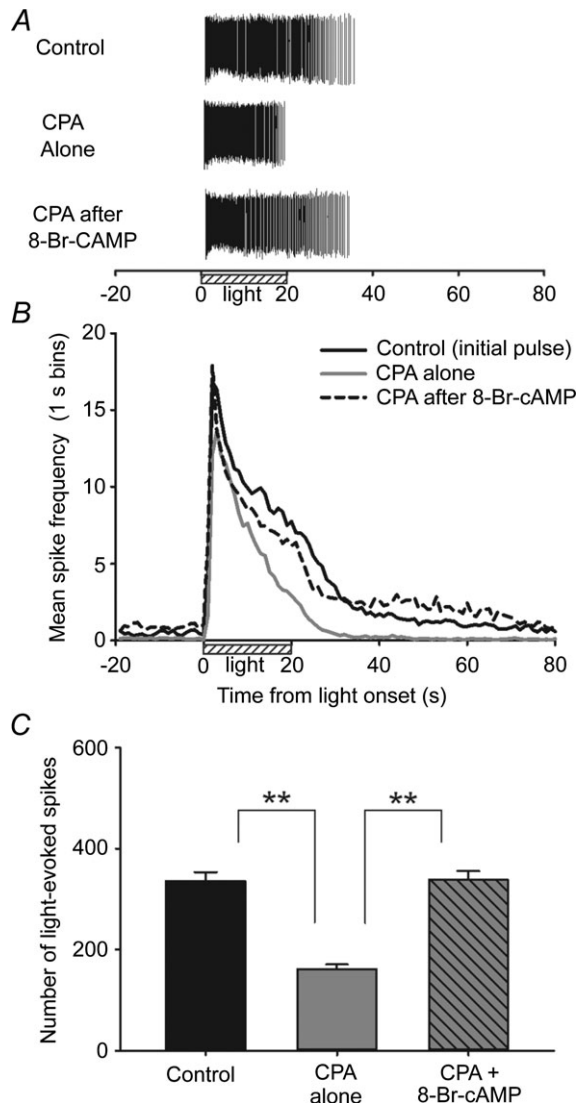
Discussion

A hallmark of ipRGC physiology is that these cells exhibit remarkably sustained spiking responses during light exposures that can persist for many seconds after the light is turned off. In this work, we demonstrate that this unique characteristic of ipRGCs is modifiable. Specifically, we identified a cAMP-dependent signalling pathway that regulates response duration, including total number of spikes fired, in light-stimulated rat ipRGCs.

Furthermore, we showed that the duration of ipRGC action potential firing evoked by bright light stimulation is significantly shortened following the activation of A_1 adenosine receptors present on these cells. This study therefore provides evidence that adenosine, a retinal neuromodulator known to influence intracellular cAMP levels, can modify the temporal properties of ipRGC light responses and alter the irradiance information that is conveyed by these photoreceptors to the brain.

Neuromodulation of ipRGCs by adenosine through cAMP-dependent pathway

The bath application of forskolin, which stimulates increased cAMP levels within retinal neurons (Dunn *et al.* 2006), significantly increased light-evoked spiking in ipRGCs recorded from either neonatal or adult rat retinas. The effect of forskolin could be blocked by pretreating retinas with inhibitors of either adenylate cyclase or PKA (using MDL 12330A and PKI-[14–22]-amide, respectively), implicating both enzymes in the pathway that mediates forskolin's actions. Consistent with the effect being cAMP-dependent, light-evoked ipRGC spiking was

significantly increased following exposure to a synthetic brominated analogue of cAMP, but not to a comparable cGMP analogue. Furthermore, treatment of the retinas with a PKA agonist (Sp-5,6-DCl-cBIMPS) affected ipRGC action potential firing in a similar fashion to forskolin, while a PKG agonist (8-pCPT-cGMP) had negligible effect. Taken together, the results indicate that an intracellular signalling cascade, which involves stimulation of PKA by adenylate cyclase-generated cAMP, influences the overall duration of light-evoked ipRGC spiking. In this regard, mammalian ipRGCs are similar to certain invertebrate photoreceptors, for which cAMP has also been shown to modulate photoresponses (Chyb *et al.* 1999; Battelle, 2002).

We next sought to identify an endogenous neuromodulator that could modify ipRGC light responses through this cAMP/PKA pathway. We assessed adenosine, known to be released in the retina at night or after dark adaptation (Ribelayga & Mangel, 2005), as such a candidate. In our experiments, bath application of adenosine (in the presence of adenosine transporter inhibitor NMBPR) resulted in a reduction in the number of light-evoked spikes fired by ipRGCs. As adenosine had the opposite effect on ipRGC light responses to forskolin,
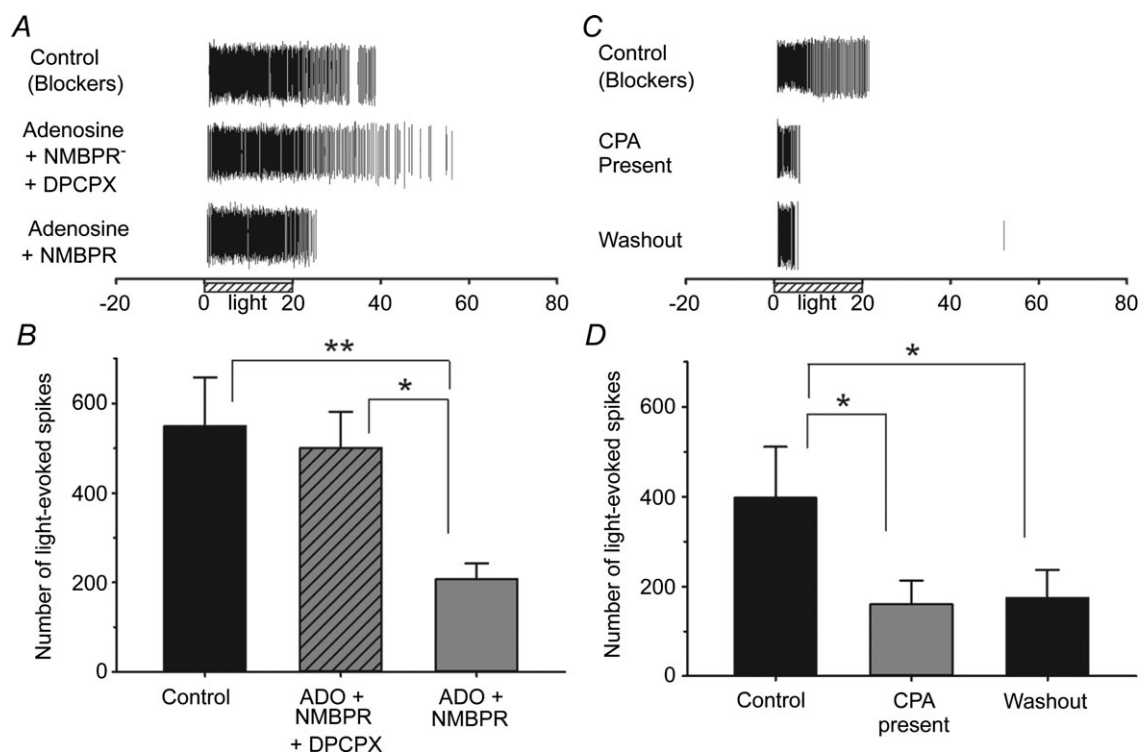

Figure 8. Adenosine A_1 receptor-mediated modulation of adult ipRGC light responses
A and *B*, example rasters (*A*) and mean spike counts (*B*) for light-stimulated ipRGCs ($N = 2$; $n = 12$) treated for 5 min with 500 μM adenosine (ADO) + 20 μM NMBPR in the presence and absence of 20 μM DPCPX. *C* and *D*, similar to ADO treatment, 5 min treatment with the A_1 receptor agonist CPA (*C*; 10 μM) reduced the total number of light-evoked spiking (*D*) in ipRGCs ($N = 4$; $n = 8$) recorded from adult (>2 months old) rat retinas. All of these recordings were performed with synaptic blocker cocktail present. **$P < 0.01$, *$P < 0.05$, one-way repeated-measures ANOVA, Holm–Sidak. Stimulus was blue light (470 nm; 3.9×10^{15} photons s^{-1} cm^{-2}).

we investigated whether the actions of adenosine were mediated through activation of A_1 adenosine receptors, which are heavily expressed in the RGC layer (Braas *et al.* 1987; Blazynski & Perez, 1991). Stimulation of A_1 receptors induces a decrease in internal cAMP levels through G_i protein-related inhibition of adenylate cyclase activity (Fredholm *et al.* 2001). In support of an A_1 receptor-based mechanism: (1) the effects of adenosine could be blocked through the use of the selective A_1 antagonist DPCPX; and (2) the A_1 agonist CPA (but not the A_3 agonist 2-Cl-IB-MECA) mirrored the effects of adenosine by reducing the duration of light-stimulated ipRGC spiking after treatment. Increasing intracellular cyclic nucleotide levels by pre-exposing the retinas to 8-Br-cAMP reversed the suppression of ipRGC photoresponses by CPA, thereby supporting cAMP-dependent signalling pathways as underlying adenosine's effect.

Similar to forskolin, adenosine significantly affected the light responses of ipRGCs from either neonatal (8–14 day old) or adult (>2 month old) rat retinas. As compounds were bath applied to the intact retina preparations, we considered the possibility that adenosine was affecting ipRGCs indirectly through its action on other retinal cells, resulting in the release of different neurotransmitters or neuromodulators onto ipRGC dendrites. However, adenosine reduced the light-induced calcium signal, which directly correlates with the number of spikes fired by these photoreceptors (Hartwick *et al.* 2007), in cultured ipRGCs that were isolated from synaptic contacts with other retinal cells. As the effect of adenosine on the immunopanned ipRGCs was blocked through co-application of the A_1 antagonist DPCPX, these experiments conclusively established that A_1 adenosine receptors are located on ipRGCs and that adenosine can directly affect these photoreceptive neurons.
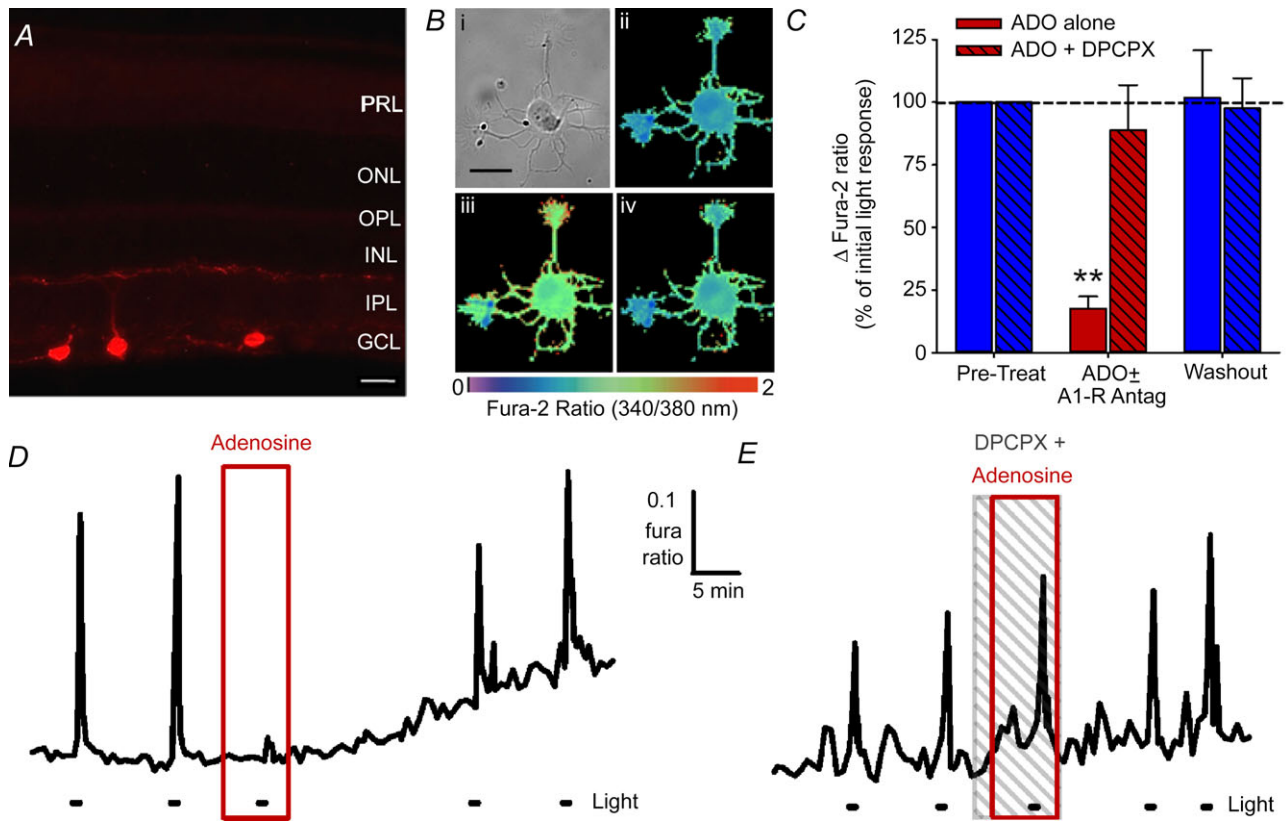

Figure 9. Adenosine inhibits light-evoked calcium responses from isolated ipRGCs in purified cultures
A, immunolocalization of melanopsin in three ipRGCs located in the ganglion cell layer (GCL) of a retinal slice from an adult rat. The primary N-terminal melanopsin antibodies used here were employed in the immunopanning procedure to generate ipRGC cultures. Scale bar = 20 μm. *B*, light evoked a rise in internal calcium levels, measured as an increase in the fura-2 ratio, in isolated ipRGCs. Example pseudocoloured images of fura-2 fluorescence ratios in (i) a cultured ipRGC before (ii), immediately after (iii) and 50 s after (iv) exposure to 20 s light pulse. Scale bar = 25 μm. *C*, data summary for the experiments involving adenosine alone ($n = 11$) and adenosine plus DPCPX ($n = 8$). **$P < 0.01$, one-way repeated-measures ANOVA, Holm–Sidak. *D* and *E*, example traces showing that adenosine (*D*; ADO; 100 μM) reversibly inhibited the light-evoked calcium signals, and ADO's effect could be blocked by adding the A_1 receptor antagonist DPCPX (*E*; 10 μM) to the bath. Stimulus was blue light (470 nm; 3.9×10^{15} photons s^{-1} cm^{-2}).

Potential downstream targets mediating adenosine's effect on ipRGC light responses

In this study, we did not examine the downstream targets of PKA that facilitate alterations in the duration of ipRGC spiking responses to light. Three possibilities that warrant future investigation include PKA-mediated phosphorylation of: (1) voltage-gated calcium channels (VGCCs), (2) canonical transient receptor potential channels (TRPCs) and (3) hyperpolarization-activated cyclic nucleotide-gated (HCN) channels.

During light exposure, calcium flows into ipRGCs through L-type VGCCs that are opened after the strong depolarization associated with action potential firing (Hartwick *et al.* 2007). Phosphorylation of L-type VGCCs by cAMP-dependent PKA is well established in the mammalian heart and skeletal muscle (McDonald *et al.* 1994; Hosey *et al.* 1996; Gao *et al.* 1997; Catterall, 2000). In the retina, adenosine has been shown to inhibit L-type VGCCs in rod and cone photoreceptors (Stella *et al.* 2002, 2007). Of particular relevance to this study, adenosine inhibits L-type VGCCs in non-photosensitive RGCs via the activation of A_1 receptors (Hartwick *et al.* 2004). VGCC-mediated calcium influx can modulate neuronal output by regulating activation of K^+ channels (Sah & Faber, 2002) and it has been previously demonstrated that adenosine induces an outward K^+ current in non-photosensitive rat RGCs (Newman, 2003). Thus, an adenosine-driven reduction in the phosphorylation of VGCCs by PKA could produce a decrease in calcium influx along with a concomitant increase in K^+ efflux. Membrane hyperpolarization would be the result of these two outcomes, leading to a reduction in spikes fired by the ipRGCs. In addition, reduced VGCC-mediated calcium influx may directly affect the primary light-gated current, as there is evidence that peak amplitude of the ipRGC photocurrent is reduced when intracellular calcium levels are lowered (Warren *et al.* 2006).

A second possibility is that adenosine-driven PKA inhibition may directly or indirectly affect TRPCs to modulate ipRGC light responses. There is anatomical and physiological evidence that a TRPC is the light-gated channel in ipRGCs (Warren *et al.* 2006; Hartwick *et al.* 2007; Sekaran *et al.* 2007). More recent evidence using conditional single- and double-gene knockout mice indicate that the initial ipRGC photocurrent is mediated through a TRPC6/7 heterodimeric channel (Xue *et al.* 2011). Consensus phosphorylation sites have been shown on TRPC proteins (Kwan *et al.* 2004), raising the possibility that stimulation of the cAMP/PKA signalling pathway could directly activate the light-gated channel. However, there is currently conflicting evidence as to whether phosphorylation of TRPC6 by PKA activates (Shen *et al.* 2011), inhibits (Horinouchi *et al.* 2012) or has no effect (Hassock *et al.* 2002) on the current carried by this channel. Further characterization of the physiological and biochemical features of TRPC6/7 heterodimeric channels (see Itsuki *et al.* 2014) is necessary to evaluate the potential effects of PKA-driven phosphorylation on their carried current.

HCN channels, which have been previously identified on ipRGCs (Van Hook & Berson, 2010), represent a third potential target for mediating the effect of altered cAMP levels on ipRGC light responses. HCN channels mediate an inward cation current that is activated at hyperpolarized membrane potentials, and typically contribute to the overall resting membrane potential and post-spiking rebound depolarization that occurs in many neurons, including other RGCs (Lee & Ishida, 2007). These channels possess cAMP-specific binding domains that modify their activation (Ulens & Siegelbaum, 2003), and dopamine-mediated increases in intracellular cAMP have been shown to shift the activation curve of HCN channels in non-photosensitive RGCs (Chen & Yang, 2007). Thus, forskolin-stimulated increases in internal cAMP levels could facilitate the opening of HCN channels, causing depolarization of ipRGC resting membrane potentials. By driving cAMP levels down via A_1 receptor activation, adenosine would be expected to have the converse effect. However, blockade of HCN channels has yet to be shown to substantially alter ipRGC light responses and it appears that a substantial hyperpolarized environment is required for ipRGC HCN channel activation (Van Hook & Berson, 2010). It remains to be demonstrated that cAMP can shift the activation curves of these channels into a physiologically relevant range.

Functional implications of adenosine-mediated neuromodulation of ipRGCs

The reduction in light-evoked spiking exhibited by neonatal and adult ipRGCs with adenosine present indicates that this endogenous neuromodulator alters the sensitivity of these photoreceptors to environmental light cues *in vivo*. Retinal adenosine levels exhibit circadian variation and peak at night (Ribelayga & Mangel, 2005), a time period that has also been associated with low cAMP levels in the ganglion cell layer (Vaquero *et al.* 2001). The source of extracellular adenosine may be from degraded ATP that is released either from glia (Newman, 2003, 2004) or from starburst amacrine cells (Neal & Cunningham, 1994; Santos *et al.* 1999). In support of the latter source, the effects of adenosine on the inner retina can be blocked by tetrodotoxin (Newman, 2005), which would be expected to affect spiking starburst amacrine cells more than non-spiking glial cells. Synaptic release of adenosine by amacrine cells may account for the absence of significant circadian changes in the inherent light sensitivity of ipRGCs as described by Weng *et al.* (2009).

In their study, ipRGC sensitivity across 24 h periods was assessed in the presence of synaptic blockers (Weng *et al.* 2009), which may have blunted the night-time rise in retinal adenosine levels and masked a circadian variation in ipRGC sensitivity that was regulated by this extrinsic neuromodulator.

Extracellular adenosine and intracellular cAMP levels are also influenced by light exposure. Prolonged dark adaptation reduces cAMP immunoreactivity in the ganglion cell layer during the subjective day while the opposite is true for light-adapted retinas (Vaquero *et al.* 2001). Similarly, dark adaptation leads to increased extracellular adenosine in the retina (Ribelayga & Mangel, 2005). While synaptically isolated ipRGCs show increases in their inherent light sensitivity following dark adaptation (Wong *et al.* 2005), similar to other photoreceptors, our data suggest that the extrinsic effects of rising adenosine levels in the dark could inhibit these cells and decrease ipRGC light sensitivity after dark adaptation *in vivo*.

As a counterbalance to adenosine, dopamine is a potential endogenous candidate for lengthening ipRGC light responses in a similar fashion to that observed in our experiments with forskolin treatment. However, it has recently been reported that activation of dopamine D_1 receptors, known to stimulate cAMP/PKA-dependent pathways (Neve *et al.* 2004), inhibited photocurrents in isolated rat ipRGCs as measured through patch voltage-clamp recordings (Van Hook *et al.* 2012). A similar inhibitory effect was noted by these authors when forskolin plus 3-isobutyl-1-methylxanthine (IBMX, a phosphodiesterase inhibitor that also acts as a non-specific adenosine receptor antagonist) was applied to voltage-clamped ipRGCs. While these findings appear to conflict with the action of forskolin described in the present study, it should be noted that this prior study reported that either forskolin or D_1 receptor agonist application had additional effects on ipRGCs that were distinct from the reduction in photocurrent. Exposure of ipRGCs to either compound caused an increase in the holding current (and decrease in input resistance) measured during voltage-clamp recordings, indicating an inward current was being activated by the treatments. In accordance with this, forskolin and the D_1 agonist induced membrane depolarization and increased background spiking when current-clamp or cell-attached (extracellular) recording techniques were employed on the cultured ipRGCs (Van Hook *et al.* 2012). This effect of forskolin on ipRGC membrane properties is consistent with the increased duration in light-evoked spiking associated with forskolin treatment found in the present study, as forskolin-induced depolarization could prolong the recovery of ipRGC membrane potential to a level below the spiking threshold for these neurons. It is therefore possible that the two disparate actions of dopamine and forskolin described by

Van Hook and colleagues are due to separate consequences of PKA activation: (1) the reduction in photocurrent is caused by phosphorylation of the melanopsin photopigment itself, as there is evidence that melanopsin can be inhibited through PKA-mediated phosphorylation when it is heterologously expressed in HEK cells (Blasic *et al.* 2012); while (2) the ipRGC depolarization is mediated by the action of PKA on ion channels such as VGCCs, TRPCs or HCN channels, as discussed in the preceding section. Although the two mechanisms appear to counteract each other, our experiments with extracellular MEA recordings indicate that the latter mechanism has a greater role in shaping the light-evoked spiking response of ipRGCs. Using neonatal and adult rat retinal flatmount preparations, our results demonstrate that an increase in light-evoked spiking is the net result associated with an elevation of internal cAMP levels within ipRGCs. As action potentials are the signals that are transmitted to the brain targets innervated by these neurons, the alteration in light-evoked spiking is the output response that would ultimately influence the functions regulated by these photoreceptors.

The inhibition of light-evoked ipRGCs by adenosine at night, or after dark adaptation, could significantly affect the photic functions that are affected by these photoreceptors, such as circadian photoentrainment, pupil constriction and alertness. Notably, adenosine has been found to act pre-synaptically at A_1 receptors to attenuate light-induced phase shifts in the suprachiasmatic nucleus, the site of the central circadian clock (Hallworth *et al.* 2002). As ipRGCs are the pre-synaptic neurons that innervate the suprachiasmatic nucleus (Hattar *et al.* 2006), the inhibition of ipRGCs by adenosine may contribute to some of the known effects for this neuromodulator on the circadian clock (Watanabe *et al.* 1996; Hallworth *et al.* 2002; Sigworth & Rea, 2003). Light signalling by ipRGCs is also thought to increase alertness (Lockley *et al.* 2006), and therefore the inhibition of ipRGC spiking at night by adenosine would be expected to promote sleepiness. With respect to pupil constriction, the contribution of ipRGCs to the pupillary light reflex is well established (Hattar *et al.* 2003; Lucas *et al.* 2003) and can be assessed in humans by measuring the prolonged pupil constriction that persists after a bright light stimulus is extinguished (Gamlin *et al.* 2007). This post-illumination pupil response (PIPR) exhibits a circadian rhythm, becoming less pronounced during the subjective night (Zele *et al.* 2011). This is consistent with our hypothesis that ipRGC light sensitivity decreases at night due to adenosinergic modulation.

ipRGCs have also been implicated in the exacerbation of photophobia that is associated with migraines, as they project to thalamic pain centres that synapse with dura-sensitive neurons (Noseda *et al.* 2010). Orange-tinted glasses that filter out blue light have been shown to reduce the frequency of migraine attacks with

short periods of usage (Good *et al.* 1991). There has also been interest in developing pharmacological treatments for photophobia that target light signalling by ipRGCs. A small-molecule antagonist of melanopsin-based photo-transduction has been recently described, and this compound reduces light aversive behaviour in rodents (Jones *et al.* 2013). As we found that adenosine modifies ipRGC light responses without fully inhibiting them, compounds that target A_1 adenosine receptors represent another therapeutic avenue to be explored for this condition. Alternatively, repeated adaptation periods in the dark may help to maximize retinal adenosine levels and reduce ipRGC signalling to the thalamic pain centres.

In summary, this work establishes an intracellular cAMP/PKA-mediated pathway that regulates light-evoked spiking in rat ipRGCs. Through this pathway, adenosine can reduce ipRGC spiking via A_1 receptor stimulation. This work suggests that the light sensitivity of ipRGCs is not a static characteristic, but instead is regulated by light- and circadian-driven changes in extracellular retinal levels of adenosine and other cAMP-related neuromodulators.

References

Battelle BA (2002). Circadian efferent input to *Limulus* eyes: anatomy, circuitry, and impact. *Microsc Res Tech* **58**, 345–355.

Belenky MA, Smeraski CA, Provencio I, Sollars PJ & Pickard GE (2003). Melanopsin retinal ganglion cells receive bipolar and amacrine cell synapses. *J Comp Neurol* **460**, 380–393.

Berson DM, Castrucci AM & Provencio I (2010). Morphology and mosaics of melanopsin-expressing retinal ganglion cell types in mice. *J Comp Neurol* **518**, 2405–2422.

Berson DM, Dunn FA & Takao M (2002). Phototransduction by retinal ganglion cells that set the circadian clock. *Science* **295**, 1070–1073.

Blankenship AG, Ford KJ, Johnson J, Seal RP, Edwards RH, Copenhagen DR & Feller MB (2009). Synaptic and extrasynaptic factors governing glutamatergic retinal waves. *Neuron* **62**, 230–241.

Blasic JR, Jr, Brown RL & Robinson PR (2012). Phosphorylation of mouse melanopsin by protein kinase A. *PLoS One* **7**, e45387.

Blazynski C & Perez MT (1991). Adenosine in vertebrate retina: localization, receptor characterization, and function. *Cell Mol Neurobiol* **11**, 463–484.

Braas KM, Zarbin MA & Snyder SH (1987). Endogenous adenosine and adenosine receptors localized to ganglion cells of the retina. *Proc Natl Acad Sci U S A* **84**, 3906–3910.

Brown TM, Gias C, Hatori M, Keding SR, Semo M, Coffey PJ, Gigg J, Piggins HD, Panda S & Lucas RJ (2010). Melanopsin contributions to irradiance coding in the thalamo-cortical visual system. *PLoS Biol* **8**, e1000558.

Catterall WA (2000). Structure and regulation of voltage-gated Ca^{2+} channels. *Ann Rev Cell Dev Biol* **16**, 521–555.

Chen L & Yang XL (2007). Hyperpolarization-activated cation current is involved in modulation of the excitability of rat retinal ganglion cells by dopamine. *Neuroscience* **150**, 299–308.

Chyb S, Hevers W, Forte M, Wolfgang WJ, Selinger Z & Hardie RC (1999). Modulation of the light response by cAMP in Drosophila photoreceptors. *J Neurosci* **19**, 8799–8807.

Dacey DM, Liao HW, Peterson BB, Robinson FR, Smith VC, Pokorny J, Yau KW & Gamlin PD (2005). Melanopsin-expressing ganglion cells in primate retina signal colour and irradiance and project to the LGN. *Nature* **433**, 749–754.

Do MT & Yau KW (2010). Intrinsically photosensitive retinal ganglion cells. *Physiol Rev* **90**, 1547–1581.

Dunn TA, Wang CT, Colicos MA, Zaccolo M, DiPilato LM, Zhang J, Tsien RY & Feller MB (2006). Imaging of cAMP levels and protein kinase A activity reveals that retinal waves drive oscillations in second-messenger cascades. *J Neurosci* **26**, 12807–12815.

Ecker JL, Dumitrescu ON, Wong KY, Alam NM, Chen SK, LeGates T, Renna JM, Prusky GT, Berson DM & Hattar S (2010). Melanopsin-expressing retinal ganglion-cell photoreceptors: cellular diversity and role in pattern vision. *Neuron* **67**, 49–60.

Ford KJ & Feller MB (2012). Assembly and disassembly of a retinal cholinergic network. *Vis Neurosci* **29**, 61–71.

Fredholm BB, AP IJ, Jacobson KA, Klotz KN & Linden J (2001). International Union of Pharmacology. XXV. Nomenclature and classification of adenosine receptors. *Pharmacol Rev* **53**, 527–552.

Gamlin PD, McDougal DH, Pokorny J, Smith VC, Yau KW & Dacey DM (2007). Human and macaque pupil responses driven by melanopsin-containing retinal ganglion cells. *Vision Res* **47**, 946–954.

Gao T, Yatani A, Dell'Acqua ML, Sako H, Green SA, Dascal N, Scott JD & Hosey MM (1997). cAMP-dependent regulation of cardiac L-type Ca^{2+} channels requires membrane targeting of PKA and phosphorylation of channel subunits. *Neuron* **19**, 185–196.

Good PA, Taylor RH & Mortimer MJ (1991). The use of tinted glasses in childhood migraine. *Headache* **31**, 533–536.

Hallworth R, Cato M, Colbert C & Rea MA (2002). Presynaptic adenosine A1 receptors regulate retinohypothalamic neurotransmission in the hamster suprachiasmatic nucleus. *J Neurobiol* **52**, 230–240.

Hannibal J & Fahrenkrug J (2004). Melanopsin containing retinal ganglion cells are light responsive from birth. *Neuroreport* **15**, 2317–2320.

Hartwick AT, Bramley JR, Yu J, Stevens KT, Allen CN, Baldridge WH, Sollars PJ & Pickard GE (2007). Light-evoked calcium responses of isolated melanopsin-expressing retinal ganglion cells. *J Neurosci* **27**, 13468–13480.

Hartwick AT, Lalonde MR, Barnes S & Baldridge WH (2004). Adenosine A1-receptor modulation of glutamate-induced calcium influx in rat retinal ganglion cells. *Invest Ophthalmol Vis Sci* **45**, 3740–3748.

Hassock SR, Zhu MX, Trost C, Flockerzi V & Authi KS (2002). Expression and role of TRPC proteins in human platelets: evidence that TRPC6 forms the store-independent calcium entry channel. *Blood* **100**, 2801–2811.

Hattar S, Kumar M, Park A, Tong P, Tung J, Yau KW & Berson DM (2006). Central projections of melanopsin-expressing retinal ganglion cells in the mouse. *J Comp Neurol* **497**, 326–349.

Hattar S, Liao HW, Takao M, Berson DM & Yau KW (2002). Melanopsin-containing retinal ganglion cells: architecture, projections, and intrinsic photosensitivity. *Science* **295**, 1065–1070.

Hattar S, Lucas RJ, Mrosovsky N, Thompson S, Douglas RH, Hankins MW, Lem J, Biel M, Hofmann F, Foster RG & Yau KW (2003). Melanopsin and rod-cone photoreceptive systems account for all major accessory visual functions in mice. *Nature* **424**, 76–81.

Horinouchi T, Higa T, Aoyagi H, Nishiya T, Terada K & Miwa S (2012). Adenylate cyclase/cAMP/protein kinase A signaling pathway inhibits endothelin type A receptor-operated Ca^{2+} entry mediated via transient receptor potential canonical 6 channels. *J Pharmacol Exp Ther* **340**, 143–151.

Hosey MM, Chien AJ & Puri TS (1996). Structure and regulation of L-type calcium channels a current assessment of the properties and roles of channel subunits. *Trends Cardiovasc Med* **6**, 265–273.

Housley GD, Bringmann A & Reichenbach A (2009). Purinergic signaling in special senses. *Trends Neurosci* **32**, 128–141.

Itsuki K, Imai Y, Hase H, Okamura Y, Inoue R & Mori MX (2014). PLC-mediated $PI(4,5)P_2$ hydrolysis regulates activation and inactivation of TRPC6/7 channels. *J Gen Physiol* **143**, 183–201.

Iuvone PM, Galli CL, Garrison-Gund CK & Neff NH (1978). Light stimulates tyrosine hydroxylase activity and dopamine synthesis in retinal amacrine neurons. *Science* **202**, 901–902.

Jones KA, Hatori M, Mure LS, Bramley JR, Artymyshyn R, Hong SP, Marzabadi M, Zhong H, Sprouse J, Zhu Q, Hartwick AT, Sollars PJ, Pickard GE & Panda S (2013). Small-molecule antagonists of melanopsin-mediated phototransduction. *Nat Chem Biol* **9**, 630–635.

Koyanagi M, Kubokawa K, Tsukamoto H, Shichida Y & Terakita A (2005). Cephalochordate melanopsin: evolutionary linkage between invertebrate visual cells and vertebrate photosensitive retinal ganglion cells. *Curr Biol* **15**, 1065–1069.

Kwan HY, Huang Y & Yao X (2004). Regulation of canonical transient receptor potential isoform 3 (TRPC3) channel by protein kinase G. *Proc Natl Acad Sci U S A* **101**, 2625–2630.

Laurenza A, Sutkowski EM & Seamon KB (1989). Forskolin: a specific stimulator of adenylyl cyclase or a diterpene with multiple sites of action? *Trends Pharmacol Sci* **10**, 442–447.

Lee SC & Ishida AT (2007). I_h Without K_{ir} in adult rat retinal ganglion cells. *J Neurophysiol* **97**, 3790–3799.

Lockley SW, Evans EE, Scheer FA, Brainard GC, Czeisler CA & Aeschbach D (2006). Short-wavelength sensitivity for the direct effects of light on alertness, vigilance, and the waking electroencephalogram in humans. *Sleep* **29**, 161–168.

Lucas RJ (2013). Mammalian inner retinal photoreception. *Curr Biol* **23**, R125–133.

Lucas RJ, Hattar S, Takao M, Berson DM, Foster RG & Yau KW (2003). Diminished pupillary light reflex at high irradiances in melanopsin-knockout mice. *Science* **299**, 245–247.

McDonald TF, Pelzer S, Trautwein W & Pelzer DJ (1994). Regulation and modulation of calcium channels in cardiac, skeletal, and smooth muscle cells. *Physiol Rev* **74**, 365–507.

Meyer-Franke A, Kaplan MR, Pfrieger FW & Barres BA (1995). Characterization of the signaling interactions that promote the survival and growth of developing retinal ganglion cells in culture. *Neuron* **15**, 805–819.

Missale C, Nash SR, Robinson SW, Jaber M & Caron MG (1998). Dopamine receptors: from structure to function. *Physiol Rev* **78**, 189–225.

Murray AJ (2008). Pharmacological PKA inhibition: all may not be what it seems. *Sci Signal* **1**, re4.

Neal M & Cunningham J (1994). Modulation by endogenous ATP of the light-evoked release of ACh from retinal cholinergic neurones. *Br J Pharmacol* **113**, 1085–1087.

Neve KA, Seamans JK & Trantham-Davidson H (2004). Dopamine receptor signaling. *J Recept Signal Transduct Res* **24**, 165–205.

Newman EA (2001). Propagation of intercellular calcium waves in retinal astrocytes and Muller cells. *J Neurosci* **21**, 2215–2223.

Newman EA (2003). Glial cell inhibition of neurons by release of ATP. *J Neurosci* **23**, 1659–1666.

Newman EA (2004). Glial modulation of synaptic transmission in the retina. *Glia* **47**, 268–274.

Newman EA (2005). Calcium increases in retinal glial cells evoked by light-induced neuronal activity. *J Neurosci* **25**, 5502–5510.

Nir I, Haque R & Iuvone PM (2000). Diurnal metabolism of dopamine in the mouse retina. *Brain Res* **870**, 118–125.

Noseda R, Kainz V, Jakubowski M, Gooley JJ, Saper CB, Digre K & Burstein R (2010). A neural mechanism for exacerbation of headache by light. *Nat Neurosci* **13**, 239–245.

Peirson S & Foster RG (2006). Melanopsin: another way of signaling light. *Neuron* **49**, 331–339.

Provencio I, Jiang G, De Grip WJ, Hayes WP & Rollag MD (1998). Melanopsin: an opsin in melanophores, brain, and eye. *Proc Natl Acad Sci U S A* **95**, 340–345.

Ribelayga C & Mangel SC (2005). A circadian clock and light/dark adaptation differentially regulate adenosine in the mammalian retina. *J Neurosci* **25**, 215–222.

Sah P & Faber ES (2002). Channels underlying neuronal calcium-activated potassium currents. *Prog Neurobiol* **66**, 345–353.

Santos PF, Caramelo OL, Carvalho AP & Duarte CB (1999). Characterization of ATP release from cultures enriched in cholinergic amacrine-like neurons. *J Neurobiol* **41**, 340–348.

Schmidt TM & Kofuji P (2009). Functional and morphological differences among intrinsically photosensitive retinal ganglion cells. *J Neurosci* **29**, 476–482.

Seamon KB, Padgett W & Daly JW (1981). Forskolin: unique diterpene activator of adenylate cyclase in membranes and in intact cells. *Proc Natl Acad Sci U S A* **78**, 3363–3367.

Seifert R, Lushington GH, Mou TC, Gille A & Sprang SR (2012). Inhibitors of membranous adenylyl cyclases. *Trends Pharmacol Sci* **33**, 64–78.

Sekaran S, Lall GS, Ralphs KL, Wolstenholme AJ, Lucas RJ, Foster RG & Hankins MW (2007). 2-Aminoethoxydiphenylborane is an acute inhibitor of directly photosensitive retinal ganglion cell activity in vitro and in vivo. *J Neurosci* **27**, 3981–3986.

Sekaran S, Lupi D, Jones SL, Sheely CJ, Hattar S, Yau KW, Lucas RJ, Foster RG & Hankins MW (2005). Melanopsin-dependent photoreception provides earliest light detection in the mammalian retina. *Curr Biol* **15**, 1099–1107.

Shen B, Kwan HY, Ma X, Wong CO, Du J, Huang Y & Yao X (2011). cAMP activates TRPC6 channels via the phosphatidylinositol 3-kinase (PI3K)-protein kinase B (PKB)-mitogen-activated protein kinase kinase (MEK)-ERK1/2 signaling pathway. *J Biol Chem* **286**, 19439–19445.

Sigworth LA & Rea MA (2003). Adenosine A_1 receptors regulate the response of the mouse circadian clock to light. *Brain Res* **960**, 246–251.

Stella SL, Jr, Bryson EJ & Thoreson WB (2002). A_2 adenosine receptors inhibit calcium influx through L-type calcium channels in rod photoreceptors of the salamander retina. *J Neurophysiol* **87**, 351–360.

Stella SL, Jr, Hu WD, Vila A & Brecha NC (2007). Adenosine inhibits voltage-dependent Ca^{2+} influx in cone photoreceptor terminals of the tiger salamander retina. *J Neurosci Res* **85**, 1126–1137.

Stellwagen D & Shatz CJ (2002). An instructive role for retinal waves in the development of retinogeniculate connectivity. *Neuron* **33**, 357–367.

Tu DC, Zhang D, Demas J, Slutsky EB, Provencio I, Holy TE & Van Gelder RN (2005). Physiologic diversity and development of intrinsically photosensitive retinal ganglion cells. *Neuron* **48**, 987–999.

Ulens C & Siegelbaum SA (2003). Regulation of hyperpolarization-activated HCN channels by cAMP through a gating switch in binding domain symmetry. *Neuron* **40**, 959–970.

Van Hook MJ & Berson DM (2010). Hyperpolarization-activated current (I_h) in ganglion-cell photoreceptors. *PLoS One* **5**, e15344.

Van Hook MJ, Wong KY & Berson DM (2012). Dopaminergic modulation of ganglion-cell photoreceptors in rat. *Eur J Neurosci* **35**, 507–518.

Vaquero CF, Pignatelli A, Partida GJ & Ishida AT (2001). A dopamine- and protein kinase A-dependent mechanism for network adaptation in retinal ganglion cells. *J Neurosci* **21**, 8624–8635.

Warren EJ, Allen CN, Brown RL & Robinson DW (2006). The light-activated signaling pathway in SCN-projecting rat retinal ganglion cells. *Eur J Neurosci* **23**, 2477–2487.

Watanabe A, Moriya T, Nisikawa Y, Araki T, Hamada T, Shibata S & Watanabe S (1996). Adenosine A_1-receptor agonist attenuates the light-induced phase shifts and fos expression in vivo and optic nerve stimulation-evoked field potentials in the suprachiasmatic nucleus in vitro. *Brain Res* **740**, 329–336.

Weng S, Wong KY & Berson DM (2009). Circadian modulation of melanopsin-driven light response in rat ganglion-cell photoreceptors. *J Biol Rhythms* **24**, 391–402.

Wong KY, Dunn FA & Berson DM (2005). Photoreceptor adaptation in intrinsically photosensitive retinal ganglion cells. *Neuron* **48**, 1001–1010.

Wong KY, Dunn FA, Graham DM & Berson DM (2007). Synaptic influences on rat ganglion-cell photoreceptors. *J Physiol* **582**, 279–296.

Xue T, Do MT, Riccio A, Jiang Z, Hsieh J, Wang HC, Merbs SL, Welsbie DS, Yoshioka T, Weissgerber P, Stolz S, Flockerzi V, Freichel M, Simon MI, Clapham DE & Yau KW (2011). Melanopsin signalling in mammalian iris and retina. *Nature* **479**, 67–73.

Zele AJ, Feigl B, Smith SS & Markwell EL (2011). The circadian response of intrinsically photosensitive retinal ganglion cells. *PLoS ONE* **6**, e17860.

Zhang M, Budak MT, Lu W, Khurana TS, Zhang X, Laties AM & Mitchell CH (2006). Identification of the A_3 adenosine receptor in rat retinal ganglion cells. *Mol Vis* **12**, 937–948.

Additional Information

Competing interests

The authors declare that they have no conflicts of interest.

Author contributions

P.S. completed experiments, analysed and interpreted data, and wrote the manuscript. A.T.E.H. designed experiments, analysed and interpreted data, and wrote the manuscript. Both authors have approved the final version of the manuscript.